INTRODUCTION

1- Crossing Rotational Bands :

The phenomenon of nuclear rotation was discovered in the early 1950s. Early experiments on Coulomb excitation as well as on alpha decay provided firm evidence for nuclear rotational motion. During the 1960s further experiments with (α,x n) reactions, as well as first experiments with heavy ions [1], including the in-beam gamma ray measurements, supplied new material for a systematic analysis of rotational motion especially at relatively high angular momenta. Many peculiar properties of nuclear rotation were discovered and understood in terms of the coupling between rotational and other nuclear degrees of freedom [2]. Simultanously with the vast increase of experimental data on high angular momentum phenomena a certain level of understanding has been achieved in the structure of the underlying nuclear motion.

In a more detailed "microscopic" description the rotational motion involves coherent contributions from many nucleons and thus referred to as a collective motion. It results in a rotation of the nucleus as a whole around an axis different from the nuclear symmetry axis. It was found that the relation between the excitation energy and spin is often a smooth one and, for spins that are not too high can be approximated by $E \sim I\,(I+1)$. The corresponding

series of states with consecutively increasing angular momentum is called a Rotational Band. The lowest state of a band is traditionally referred to as a Band Head. Many states of different intrinsic structure can in principle become band heads.

The band built on the ground state of the nucleus is referred to as the Ground-State-Band. All other bands are called excited or Side-Bands. The lowest energy state of a given angular momentum is called the Yrast state. The sequence of all Yrast states is called the Yrast line (Swedish : Yr "dizzy", "yrast" the dizziest) [3].

The coupling of intrinsic and rotational degree of freedom in nuclei and the evolution of the nuclear structure as a function of rotational as a rotational frequency has been a major issue in nuclear physics for several decades [2].In particular, the characterization of the superfluid-to-normal phase transition induced by the rotation (analogous to the one induced by a magnetic field in a bulk superconductor) continuous to attract the attention of high-spin spectroscopists [4]. In a finite system like the nucleus this phase transition does not seem to occur abruptly but rather in a stepwise way which can be thought of as a band crossing phenomenon [5].

Level crossing phenomena play an important role in nuclear structure. They usually occur when one studies the

pattern of single-particle excitations as a function of collective parameters characterizing the mean field, in which the nucleus move. As the nucleus rotates faster and faster the paired ground state band is crossed by an excited two-quasiparticle structure called the S-band [6], in which a significant part of the total nuclear spin is the angular momentum of the two particles aligned with the rotation axis. It is energetically cheeper for the nucleus to break a pair and in so doing to achieve a decrease in the rotational energy [5]. A very famous case is the Back-bending phenomenon, which was discovered [6] in rotating rare-earth nuclei and has since been studied in great detail in many regions of the periodic tables. It has been understood as the crossing between the superfluid ground-state band and a Coriolis decoupled rotational band based on states for which only one pair of nucleons is broken i.e., the so called two quasiparticle (2qp) states. The Coriolis force favors alignment of the angular momentum of the unpaired nucleons along the axis of rotation [6]. This process can continue through the breaking of additional pairs until, eventually,an essentially pairing free regime will be reached.

In the rare-earth region the first pair to break ("decouple") is a pair of $i_{13/2}$ neutrons occupying low-Ω states in the deformed field (Ω is the projection of the particle angular momentum on the symmetry axis). Since the

quantal collective rotation is about an axis perpendicular to the symmetry axis these high-j, low-Ωparticles are the most easy ones to decouple from the deformation field and to align with the rotation axis. This can be viewed as an effect of the Coriolis force acting in the rotating frame of the nucleus. It is natural to expect similar behaviour for particles in other high-j-orbitals. In addition, negative parity decoupled 2qp bands are expected to occur at similar energies to the positive-parity 2qp bands.

2- Quasiparticle Configuration :

2.1- Basic Concepts :

The high angular momentum states carry the information on the role of superfluid correlations existing among nucleons and,in particular, on a possible phase transition in the nucleus from the superfluid to the normal phase.The precise theoretical description of such a phase transition and of the physical effects characteristic of its manifestation are among the interesting, presently unsolved questions on nuclear structure [3]. Among the theoretical approaches, the independent quasiparticle description of rotational bands is at present a powerful tool for interpreting a broad class of high spin phenomena. The independent quasiparticle description promises a degree of generality analogous to that of the Nilsson model which was introduced in 1950s to interpret single-particle excitation.

The rotation of a nucleus about an axis that does not overlap with the symmetry axis induces coupling between the individual nucleonic orbitals and the rotational degrees of freedom of the average nuclear field. This coupling, which tends to align partially each of the nucleonic angular momenta, may be regarded as an effect underlying most of the important phenomena in the domain of rotational excitations.

In order to gain a first insight into the properties of rotating nuclei a description of nuclear rotation in terms of classical motion may be employed as a zeroth approximation. The nucleus is then thought to have a structure analogous to that of a rotating drop of matter, with its dynamical properties represented by surface tension and the Coulomb energy coefficients.These coefficients are adjusted in order to represent the properties of nuclear matter [3]. In order to account for collective rotation around an axis perpendicular to the symmetry axis the procedure suggested by Inglis [7,8], known as the cranking model approximation is frequently employed.

2.2- Cranking :

The nuclear field is rotated externally with constant angular velocity about a fixed axis. The rotation of an average field V, unsymmetric with respect to the rotation axis, introduces an explicit time dependence to the Schrödinger equation. This may, however, be reduced to

a stationary equation of motion when the laboratory frame (x y,z) is transformed into the rotating frame (x',y',z'): x' = x, the x-axis is chosen as rotation axis.

y' = y cos wt + z sin wt, z' = -y sin wt + z cos wt

transforming the original time-dependent Schrödinger equation.

$$i\hbar \frac{\partial \Psi_{lab}}{\partial t} = H_{lab} \Psi_{lab} \qquad (1.1)$$

Ψ_{lab} and H_{lab} referring to a nonrotating laboratory coordinate frame, by means of the rotation operator [3].

$$\mathcal{R} = e^{-iJ_x wt}$$

Where $J_x = J_{x'}$ denotes the x-component of the total angular momentum, we obtain

$$\Psi_{lab} = \mathcal{R}\, \Psi_{intr.} \quad \text{and} \quad H_{lab} = \mathcal{R} H_{intr} \mathcal{R} \qquad (1.2)$$

The quantities $\Psi_{intr.}$ and $H_{intr.}$ refer to the body fixed (rotating, intrinsic) coordinate frame. By subistituting equations (1.2) into (1.1),

$$i\hbar \frac{\partial \Psi_{intr.}}{\partial t} = \left(H_{intr.} - \hbar \omega J_{x'} \right) \Psi_{intr.} \qquad (1.3)$$

Equation (1.3) is stationary, since the potential entering $H_{intr.}$ is now expressed in the rotating coordinate frame (x', y', z') and thus does not depend explicity on time [3].It is assumed that the average field V is not affected by rotation. The second term on the right-hand side of eq. (1.3) is in analogy to the Coriolis and centrifugal forces in classical mechanics.

Equation (1.3), may be written as

$$i\hbar \frac{\partial \psi_{intr.}}{\partial t} = H^{\omega} \psi_{intr.} \qquad (1.4)$$

Where

$$H^{\omega} = H_{intr.} - \hbar\omega J_{x'} \qquad (1.5)$$

is called a Cranking Hamiltonian or Routhian [3]. Since H does not depend on time, the solution to equation (1.5) can be reduced to the eigen value problem of H^{ω}. In particular if H describes a system of independent particles, then so does H^{ω}, because $J_{x'}$ is a one-body operator.

The Cranking Hamiltonian, describes the dynamical coupling of the intrinsic nuclear degrees of freedom with those characterizing nuclear rotation.

2.3- The Independent Quasiparticle Method and Collective Rotation :

Within the last twenty years the well-known Hartree-Fock-Bogolyubov (HFB) formalism has been applied to the description of nuclear rotation after employing the cranking-model procedure [9,10,11]. This formalism known also as the HFBC (HFB cranking) leads to a description of a rotating nucleus in terms of elementary excitations, the so-called independent quasiparticle energies (Routhians). The HFB treatment of H^{ω} (the cranking Hamiltonian) leads to the quasiparticle equations in the rotating system.

deformation (ϵ_2 and ϵ_4) described sufficiently well the nuclear distortions of fast rotating nuclei along their Yrast line. In most cases, it is invariant with respect to space (parity invariance), $[H^{\omega}, \mathcal{P}] = 0$, from which it follows that the solution to the HFBC equation can be denumerated by the parity quantum number $\pi = \pm 1$.

The other symmetry that remains, in addition to the parity symmetry, is the invariance of H^W with respect to the rotation $\mathcal{R}_{x'} = e^{-i\pi J_{x'}}$. The square of this operator is equivalent to a rotation of the system through the angle 2π. Thus we can write: $(\mathcal{R}_{x'})^2 = (-1)^A$ [3], A denotes the total number of particles. Introducing r, the eigen values of $\mathcal{R}_x$ is called the signature [3] $r = (-1)^I$ where I denotes the total nuclear spin. Thus for systems with an even number of nucleons we have

$r = +1 \quad (\alpha = 0), \quad I = 0,2,4, \ldots\ldots$

$r = -1 \quad (\alpha = 1), \quad I = 1,3,5, \ldots\ldots$

while for system with odd particle number,

$r = -i \quad (\alpha = +1/2), \quad I = 1/2, 5/2, 9/2, \ldots\ldots$

$r = +i \quad (\alpha = -1/2), \quad I = 3/2, 7/2, 11/2, \ldots\ldots$

The above four relations can be cast into one equivalent expression : $I = \alpha \bmod 2$

It also follows that the particle number fulfills the relation : $A = 2\alpha \bmod 2$.

The classification of single-particle states by means of the signature quantum number proved to be, like parity, an important tool for identify the nucleonic orbitals in the rotating nuclear potentials [3].The rotation-sensitive orbitals are found to be the lowest members of high-j multiplets, such as :

$h_{11/2}$ (1/2), $h_{11/2}$ (3/2) ..... or

$i_{13/2}$ (1/2), $i_{13/2}$ (3/2) .....

In Nilsson notation

(550 1/2), (541 3/2) ..... or

(660 1/2), (651 3/2) ..... respectively.

2.5- Representation of the Quasiparticle Configuration :

The quasiparticle states $|\alpha\mu>$ can then be classified with respect to the parity π and the signature α. In the case of single particle states, α takes the value $\pm$ 1/2.

The numerical solutions (Eq. I) can be presented in diagrams showing $é_{\alpha u}(\omega)$, which are referred to as quasi-particle energy diagram. Fig. (a), shows a diagram of the quasiparticle levels as function of the angular frequency. For each quasiparticle state, there is a conjugate state with signature and energy having opposite signs.

The quasiparticle trajectories in the diagram have been computed as a function of the ratio ω/ω_0 of the rotational to the harmonic oscillator frequencies. In

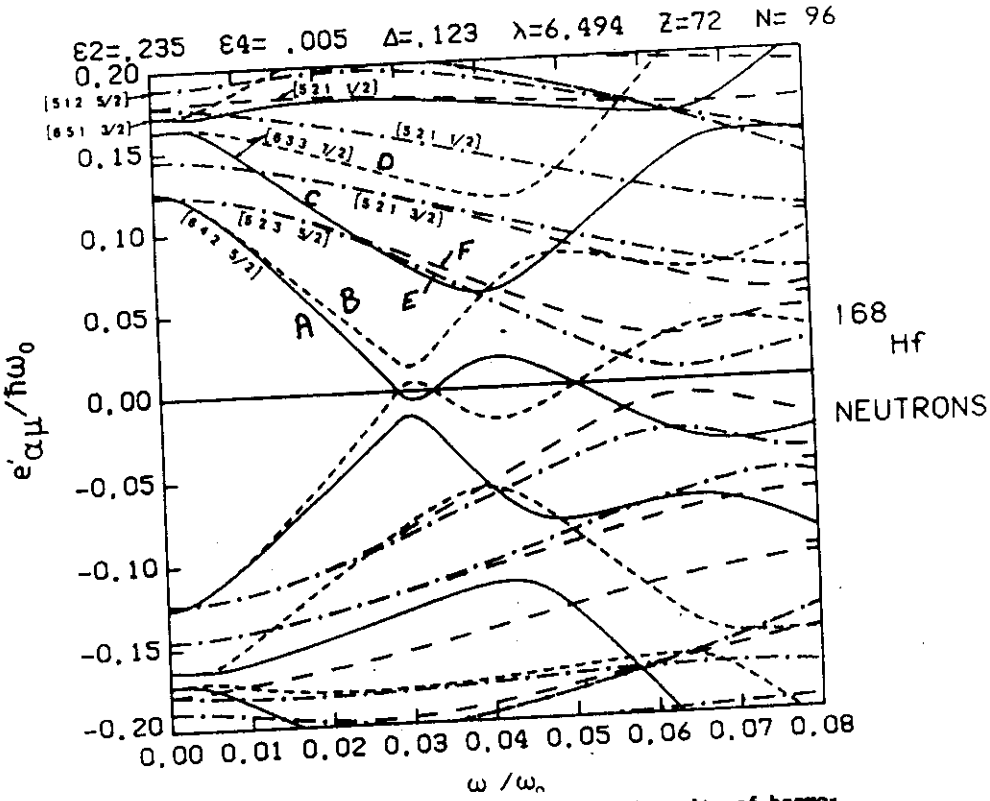

Fig. a : Quasiparticle energies, expressed in units of harmonic oscillator energy $\hbar\omega_0$, plotted as function of the rotational frequency in units of the oscillator frequency ω_0. [14]. The solid and short dashed curves represent $\pi,\alpha = (+,+\,1/2)$ and $(-,-1/2)$ respectively, while the dash dot and long dashed curves represent $(-,+1/2)$ and $(-,-1/2)$ respectively. A,B,C,D,.. refer to trajectories constructed for the $i_{13/2}$ orbits.

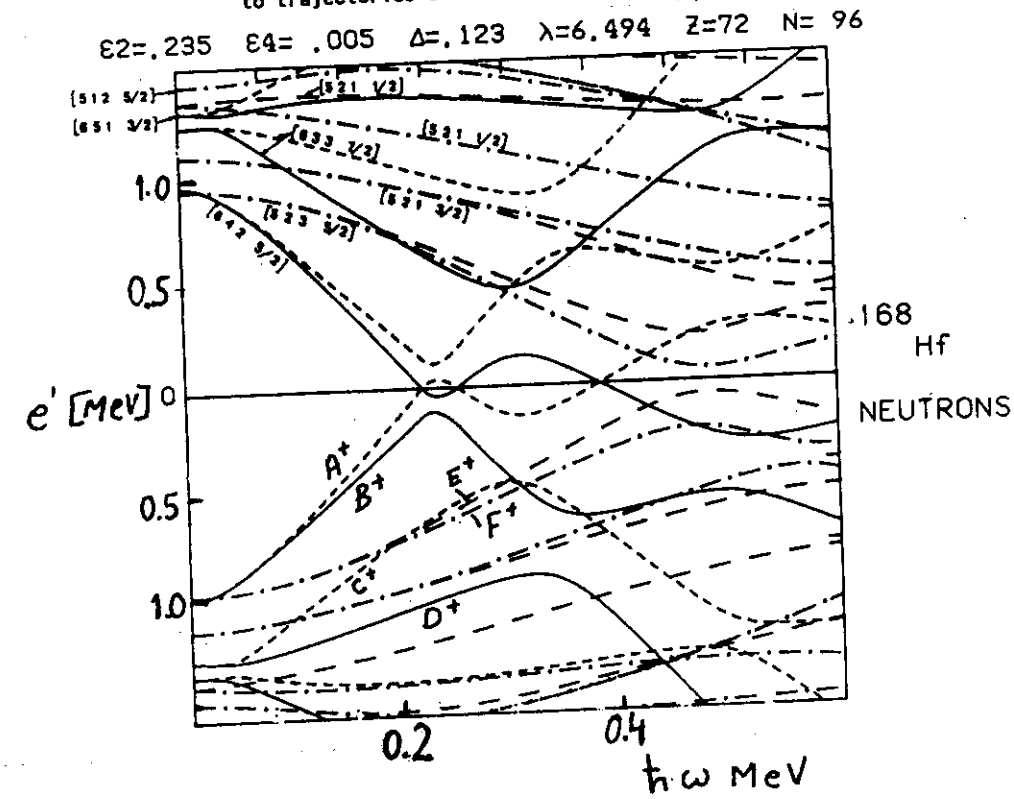

Fig. b : Quasineutron trajectories for N=96 nucleus ^{168}Hf. The energies and the rotational frequency are given in units of Mev.

analyzing experimental data, it is necessary to choose a numerical value for ω_o . The usual choice for a nucleus of mass number A is,

$$\hbar\omega_o = 41\ A^{-1/3}\ [1 \pm \frac{(N - Z)}{3A}]\ \text{Mev} \qquad (1.8)$$

Where the minus sign is to be used for protons and the plus sign for neutrons. The quasiparticle trajectories shown in (Fig. b) have been redrawn as a function of hw using Eq. (1.8) to facilitate comparison with experimental data.The energy levels are distinguished in the plots [14] according to their symmetry quantum numbers, parity π and signature α, by the style of the lines and are labeled in addition with the Nilsson quantum numbers $(Nn_2 \Lambda \Omega)$ of the axial harmonic oscillator for complete classification. The Nilsson quantum numbers are of immediate relevance only for $\omega = 0$. When ω grows the states become more or less mixed. In cases where two states with the same π and α are almost degenerate at $\omega = 0$, there may occur a strong mixing even at small .

Letter labels is an alternative prescription for labeling the quasiparticle levels. The four first levels of the high-j intruder shell ($h_{11/2}$ protons or $i_{13/2}$ neutrons) above the Fermi surface are labeled A,B,C and D while the levels of the opposite parity are labeled (E,F,C ..... The conjugate levels are labeled A^+, B^+, ...etc.

2.6- The Aligned Angular Momentum, i :

The projection of the angular momentum onto the x-axis (rotational axis) is called the aligned angular momentum. It is equal to the negative slope of the quasiparticle trajectories

$$i_{\alpha\mu} = \frac{-d\, e_{\alpha u}(\omega)}{d\,\omega} \qquad (1.9)$$

2.7- Two-Quasiparticle Configurations :

The vacuum configuration of an even nucleus is given by the corresponding diagram with all negative energy quasiparticle states filled. In the occupation number representation for quasiparticle, configurations for adjacent add nuclei and excited-state configurations in even nuclei are constructed by placing one or more quasiparticles into unoccupied states, subject to the following conditions [14]

i- If a state $|\alpha\mu\rangle$ is occupied the conjugate state is free.

ii- Out of a conjugate pair only one of the states contributes to the excitation energy, aligned angular momentum, signature, parity, and other quantities.

The quasiparticle diagrams are used to calculate excitation energies and other quantities relative to a reference configuration. One may consider this reference as the vacuum for a set of quasiparticles defined by only

those quasiparticle states that are free in the vacuum configuration. All other quasiparticle configurations are then generated from the reference by placing additional quasiparticle into these free levels according to the ordinary Fermi statistics of quasiparticle (the number is not conserved, and excitation energy is equal to the sum of the quasiparticle energies), with the states which are occupied in the reference configuration disregarded completely[14].The display of the full set of solutions ensures the freedom of choice of the reference configurations.

Relative to the reference configuration, excitation energies are given by the sum of the energies of the additional quasiparticles. The corresponding gain in aligned angular momentum is given according to Eq. (1-9) by the sum of the slopes of the trajectories occupied by the additional quasiparticles. Multiquasiparticle configurations are described by indicating the labels of all the excited quasiparticles. A number of frequently used labels for the neutron system are listed in table A:

Table (A): Examples of different types of labels used for two-Quasiparticle configurations.

Individual π and α Labels	Total π,α Labels	Letter Labels
-	$(+, 0)_1$	Vacuum
$[(+, 1/2)_1 \ (+, -1/2)_1]$	$(+, 0)_2$	(AB)
$[(+, 1/2)_1 \ (-, 1/2)_1]$	$(-, 1)$	(AE)
$[(+, 1/2)_1 \ (-, -1/2)_1]$	$(-, 0)$	(AF)

Consider a nucleus deexciting along its yrast line. If in a certain spin range two rotational bands cross at the yrast line, it is equivalent to say that the nucleus changes its intrinsic structure. This corresponds to a transition from one band to the other (Fig. c). The situation of a sharp crossing is illustrated in (Fig. c). It can immediately be seen that the angular velocity of rotation which is related to the slope of the curve of E vs I [$\omega(I) = \frac{1}{\hbar}\frac{d E (I)}{d I_x}$] must decrease at the corrsing point I= I_{cross}, whereas I increases. This means physically that a part of angular momentum is transferred into the intrinsic degrees of freedom, thus leading to a slowing down of the collective rotation.

The graphical representation of the band crossing effect looks much more dramatic if ω instead of I as an independent variable.In such representation all the important physical quantities-energy, angular momentum, aligned angular momentum, moment of inertia,etc.exhibit a multivalued behaviour; the latter was discovered experimentally for the first time by **Johnson et al. [6]** and is often called a backbending effect. Fig.(c-2) shows that a strong interaction ("repulsion") between the bands may smooth out the dramatic effect of band crossing [3].

Fig. (c):
Band Interaction.

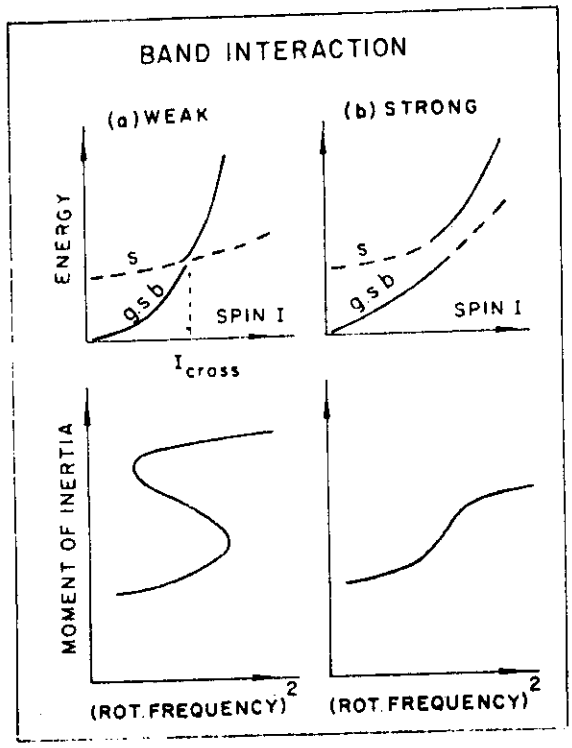

Typical examples of nuclei exhibiting such a collective rotation with crossing bands are provided in the regions of mass number $150 \leq A \leq 190$ (partly overlapping with the rare-earth region) and $A \geq 220$ (Actinide region).

It is by now customary to distinguish between the types of moments of inertia [16,17,18] often designated as $\mathcal{J}^{(1)}$ and $\mathcal{J}^{(2)}$. The first moment of inertia $\mathcal{J}^{(1)}$ is related

to the first derivative, or the slope, of the level energy E vs I^2 curve. $\mathcal{J}^{(1)}$ referred to as the "kinematical" or "static moment of inertia. The second moment of inertia $\mathcal{J}^{(2)}$ is related to the second derivative, or the curvature of the E-I curve. $\mathcal{J}^{(2)}$ is called the "dynamical" moment of inertia. The static and dynamic moments of inertia can be deduced from knowledge of discrete-line transitions in aligned band. The simplest definition of the static moment of inertia is then [19].

$$\mathcal{J}^{(1)} = \frac{I_x}{\omega} = \frac{i}{\omega} + (\mathcal{J}_o + \mathcal{J}_1 \omega^2) \qquad (1.10)$$

Which makes it equivalent to the VMI model [variable moment of inertia [20]). This is half the usual effective moment of inertia, $2\mathcal{J}/\hbar^2 = (4I - 2)/E_\gamma$ for an I --> I-2 transition. The confusing effect of the alignment term in $\mathcal{J}^{(1)}$ can be eliminated by defining $\mathcal{J}^{(2)}$ as :

$$\mathcal{J}^{(2)} = \frac{dI_x}{d\omega} = \mathcal{J}_o + 3\,\mathcal{J}_1 \omega^2 \qquad (1.11)$$

$\mathcal{J}_o$ and $\mathcal{J}_1$ are the two parameter Harris formula [21].

4- VMI-Simple Model :

Many attempts have been made to provide a theoretical description for the anomalous behaviour of the moment of inertia at high spin in nuclear rotational bands of medium and heavy nuclei.The variable moment of inertia (VMI)model [20] and its phenomenological equivalent, the Cranking (CSM) model [21], have been generally accepted as giving very good descriptions of ground state bands, and also

side bands (β and γ bands), of even-even nuclei up to the point where backbending occurs.More recently,Kelin and his associates [22,23,24] have proposed two generalization of the VMI model. Both modify the I (I+1) dependence (the rotational energy term) in VMI model.

A simple model for backbending [25], as proposed, gives a very accurate description of all ground state, β or γ bands of medium and heavy nuclei where the effect has been observed. The same set of VMI parameters are used for both the ground state band and the superband (S-band), since it has been experimentally found that the moment of inertia of the nucleus after the backbending point remains almost constant, suggesting a superband of purely rotational nature [26]. The two bands are coupled through the general band coupling formalism [2], involving either an angular momentum dependent interaction term, or a constant interaction term. Since it is widely admitted that backbending occurs only when the interaction between the two bands is small (usually less than 50 Kev [27,28,29], it is expected that the interaction term have an important effect only on the one or two levels closest to the point of band crossing, the rest of the levels remaining practically unaffected. This suggest that the two-band coupling is always enough and no multiband coupling caculations are necessary even in cases where multiple band corssings occur, except in the rare case where three or more bands meet at the same point [25].

5- Previous Work :

Spectroscopy of high-spin states began in the well deformed rare-earth nuclei [30,31,1]. These nuceli have the experimental "advantage" of exhibiting rotational band structure with transitions having large E2 strength connecting the states of spin I and I-2. More recently the heavier rare earths have been well studied [32,33,34] and understood in the framework of the cranked shell nodel.

It is interested to study some properties of high spin states in even Hf isotopes (162,164,166 and 168).

$^{162}_{72}Hf_{90}$:

It is the lightest Hf isotope studied to date. Excited states in ^{162}Hf were investigated up to spin $I \simeq 38$ using the anti-compton spectrometer array HERA with 21 detectors. These states were populated in the reaction $^{126}Te(^{40}Ca,\alpha n)^{161,162}$ Hf [35]. The assignments for the positive-parity yrast sequence are given up to 40^+. Number of transitions are assigned as the continuation of the ground band beyond the first band crossing. Assignments for the negative-parity side-bands (AE-ABCE) and (AF-ABCF) are given up to 29^- and 24^- respectively as in the unique available published ref. [35]. The results are interpreted within the framework of the cranked shell model.

$^{164}_{72}Hf_{92}$

High-spin states in ^{164}Hf were populated in the reactions $^{148,150}Sm$ ($^{20,22}Ne$, xn) $^{163-166}Hf$ with $^{20,22}Ne$ beams of 106-117 Mev [33] the yrast line is observed up to [11162 Kev (34^+)]. The states up to (8433.4 Kev 28^+) have been populated using the reaction ^{120}Sn (^{48}Ti, 4n)^{164}Hf [36]. States in the two negative-parity-side bands (-,0) and (-,1) are given up to 10 Mev in excitation energy [33,36]. These two previously works are published in the same year (1987). The spin assignments to some states are in disagreement and some transitions are missed.

The [1512 Kev (5^-)] assigned as the lowest member of the (-,1) band which extends up to 31^-[33].The same energy level is assigned as the lowest member of the (-,0) band with spin 4^- [36]. The results are interpreted within the framework of the (CSM) model.

$^{166}_{72}Hf_{94}$

The yrast band (+,0) and one side band were known previously up to 22^+ and 21^- states, respectively [37]. The energy levels for both g.s and S-bands were predicted upon the principles of variable moment of inertia model (VMI) and variable anharmonic vibrator model (VAVM) [38]. Extensions of (+,0) and (-,1) bands to appreciably higher spins are reported [33]. In addition, a second-negative-parity side band (-,0) up to [9991 Kev (32)] is identified [33].

$^{168}_{72}Hf_{96}$:

The yrast sequence [39] in ^{168}Hf has been extended to (10549.6 Kev 34^+) and two negative-parity-side-bands have been observed to 33^- and 30^- [40,41]. The states have been established by measuring $\gamma - \gamma$ coincidence following the reactions ^{124}Sn (^{48}Ti,4n) and ^{156}Gd (^{16}O, 4n). The nucleus ^{168}Hf was studied up to [12741.6 Kev (38^+)] in the yrast band and to [14344.8 Kev (41^-)] and [12932.5 kev (38^-)] in the lowest two negative-parity bands. The order of some transitions in the ground band was found to reversed from [40] but ingreement with [39]. A new band with even spins and negative parity was identified. This new band built on (1813.3 Kev 6^-) and extended up to [7425.3 Kev (26^-)][41].

The study of high-spin states in deformed doubly even nuclei, has for some years been mainly concentrated on the ground state rotational bands [42]. The role of the β and rotational bands in the phenomenon of backbending in the ground state band (g.s.b) has been recognized [43]. Models have developed, and in particular the variable moment of inertia (VMI) model [20], which attempt to describe, in a unified way, the g.s.b and other bands. Finally,increasing interest has arisen on the properties of the negative-parity bands which can also be described by the VMI model [22,23,25,44], as well as by other theories [45] All these calculations yield detailed predictions on the energy and decay properties of the various members of these side bands.

II-1- The VMI-Model :

The two-parameter variable moment of inertia model (VMI) [20] and its phenomeological equivalent,the Cranking model [21], have achieved a permanent status for the representation of the energies of ground-state bands of deformed nuclei below the region of band crossing. Thus it is interesting to extend the VMI-model above the band crossing, and to see how it can be used for both positive parity and negative parity bands. The interest is at least on two accounts :

i- The VMI-model uses two parameters (the ground-state moment of inertia $\mathcal{I}_0$ and the restoring force constant

For the side band where the moment of inertia remains almost constant

$$E_S(I) = E_o + A\,[I\,(I+1) - K^2] \qquad (2.5)$$

where E_o is the bandhead energy and A is the inverse of the constant moment of inertia $A = \frac{\hbar^2}{2\mathcal{J}_o}$ and K is the band configuration.

The four independent parameters C, $\mathcal{J}_o$, E_o and A are the model parameters, fixed by fitting four of the experimentally known levels of the band.

Moment of Inertia :

The anomolous behavior of the moment of inertia of high spin in nuclear bands of medium and heavy nuclei can be revealed in the most sensitive backbending plot of the conventional $2\mathcal{J}/\hbar^2$ versus $(\hbar\omega)^2$ curve with

$$2\mathcal{J}/\hbar^2 = \frac{4I - 2}{E_I - E_{I-2}} \qquad (2.6)$$

and

$$(\hbar\omega)^2 = \left[\frac{E_I - E_{I-2}}{(I\,(I+1)^{1/2} - [(I-2)\,(I-1)]^{1/2})}\right] \qquad (2.7)$$

It is of interest to follow the high spin properties from the weakly deformed lighter ^{162}Hf isotope up to the strongly deformed one ^{168}Hf.

II.2- Observed Bands in ^{162}Hf :

^{162}Hf is the lightest Hf isotopes studied to date. It lies far from the line of stability and is only weakly deformed with R_{42} = 2.56 (Transion region 1).

A- The Energy Spectrum

The observed levels of ^{162}Hf can with few exceptions be calculated as members of rotational bands. Plots of these bands in E_x versus I(I+1) space are shown in (Fig.1)

A.1- Positive Parity Levels :

The positive-parity yrast sequence in ^{162}Hf has been observed up to [14:178 MeV (40^+)][35], extended beyond the first and second band crossings. The ground-state band is excited to spin 10g,i.e up to the backbending region since the energy of the 12^+ - 10^+g transition (550 KeV) is lower than the 10^+g - 8^+g transition (695.3 KeV).

The sideband (s.b.) extended from (3.185 MeV 12^+_s) up to the second crossing and continue to the last two states [13.101 MeV (38^+) and [14.178 MeV (40^+)] which are regarded as tentative [35].

A sequence of states begining with the 3.997 MeV level has been observed and tentatively assigned as even spin [from (14^+) ---> (20^+)] and positive parity, as BC band.

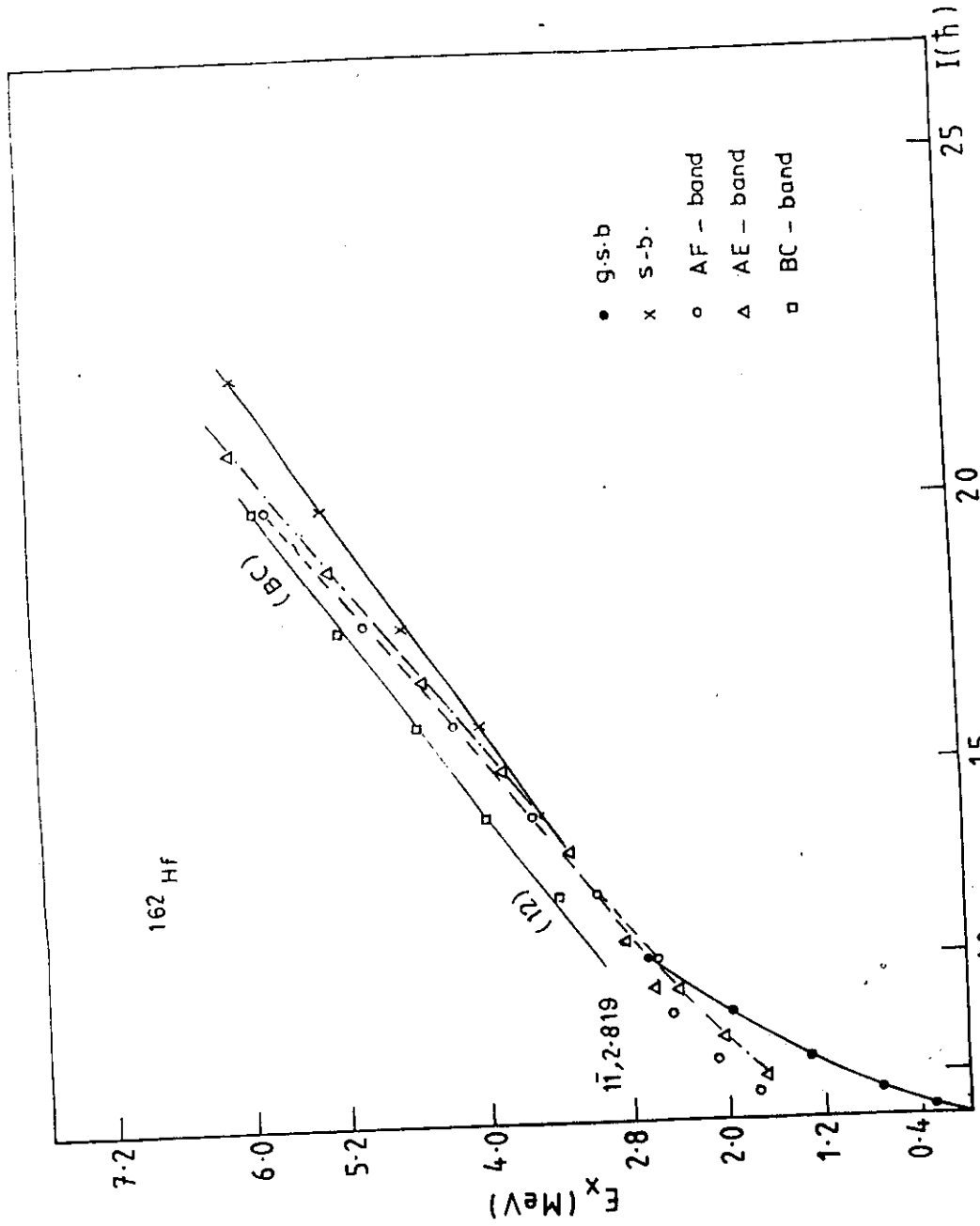

Fig. 1: Various Bands of ^{162}Hf Plotted as E_x Versus I (I+1)

The level 3.386 MeV (12^+) is considered as the begining of this band due to its position in E_x versus I(I+1) space (Fig. 1).

A.2- Negative Parity Levels :

The states in the two negative parity sidebands (-,0) and (-,1) are taken from ref. [35]. The (-,0) band begining with the 1.735 MeV, 4^- up to 5.777 MeV, 20^-. The two highest 6.595 MeV and 7.423 MeV levels, beyond the band crossing, regarded as tentative with spins (22^-) and (24^-), respectively. The systematic occurrence of even-and odd spin negative parity bands in the neighbouring nuclei make spins 6^- and 8^- most likely for the 2.118 and 2.439 MeV levels. The remaining levels were assigned as members of this band based on the positions in E_x versus I(I+1) space. The (-,1) band begining with the 1.648 MeV, 5^- up to the 9.185 MeV (29^-) beyond the band crossing. The results of the angular correlations measurements make spins 9^- for the 2.489 and 2.576 MeV states [35]. In the present analysis, the 2.489 Mev, 9^- is on the smooth curve through the (-,1) band members. The neighboring 9^-level of 2.576 MeV lies well above it.

B- The Predicted Energy Levels

The band grouping is well exhibited on the E_x versus spin-I plot in (Fig. 2). The energy levels of such transitional nucleus ^{162}Hf is well represented by the cubic polynomial [46].

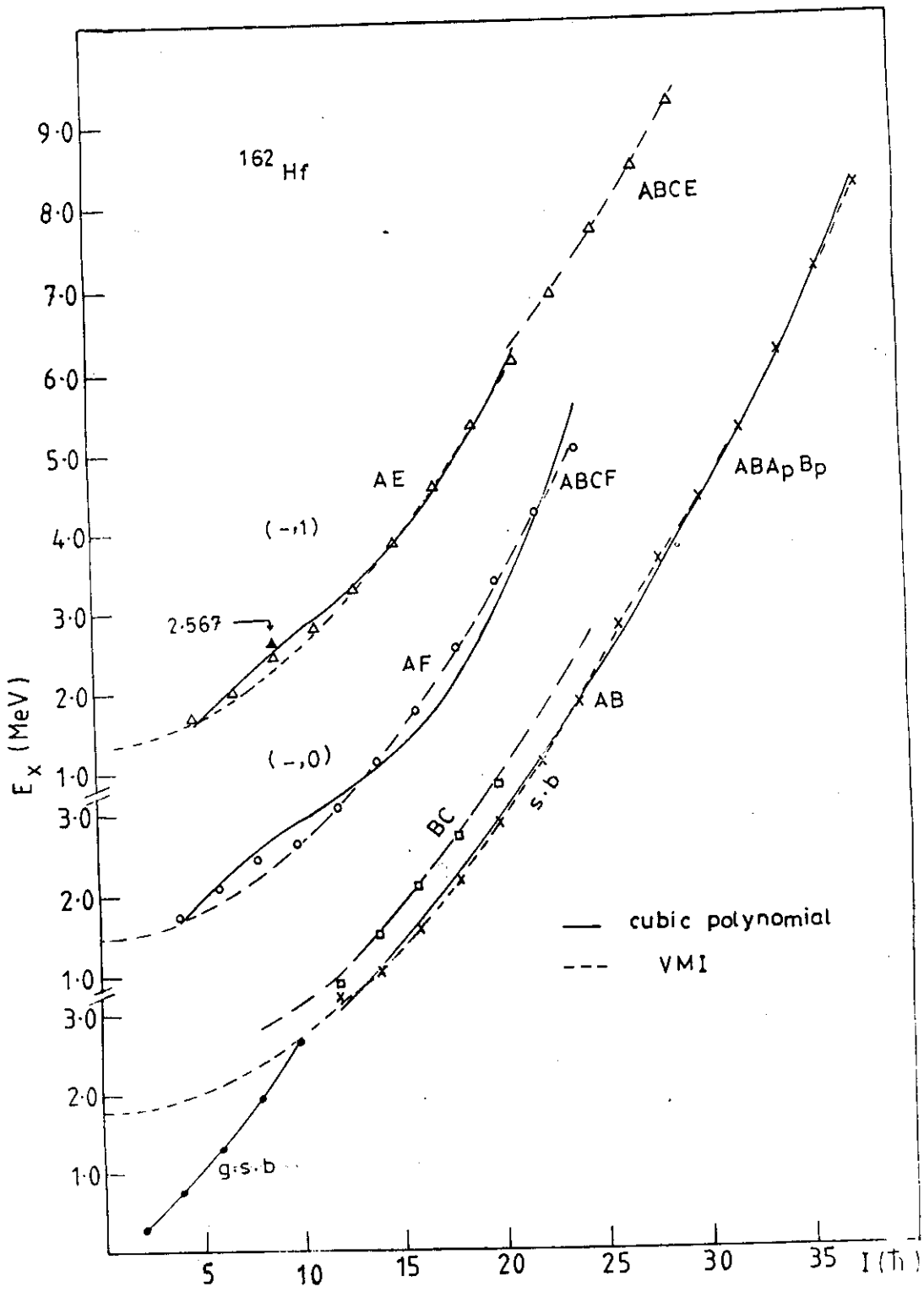

Fig. 2: Plot of the level excitation energies (E_x) as a function of spin I for various bands in ^{162}Hf connected by a theoretical curves.

$$E_I = a\ I + b\ I^2 + CI^3 \qquad (2.8a)$$

$$= (a-b)I + bI\ (I+1) + CI^3 \qquad (2.8b)$$

and the cascade γ-ray energies by

$$E = A + BI + CI^2 \qquad (2.9)$$

where A,B,C are related to a,b,c. In order to find the relative contribution of the vibrational and rotational terms in (2-8b), the least square fitting is applied to the cascade E using Eq. 2.9 for: the g.s. band ($I \leq 10^+$) below the backbend, the S. band (AB ---> ABApBp) ($12^+ \leq I^\pi \leq 40^+$) below and above the second backbend, the (-,0) band (AF ---->ABCF) [(4^-) $\leq I \leq 24^-$) and (-,1) band (AE-->ABCE) ($5^- \leq I \leq 21^-$). Table (1) lists the values of the parameters a,b,c. The vibrational structure of the bands is reflected in the larger value of the parameter "a", with b/(a-b) in Eq. (2-8b) at only 34% in the g.s. band. It is reflected again in the much larger value of "a", with b/(a-b) at 0.1%, 6% and 5.5% in the other three bands, [(s.b, (-,0) and (-,1)] respectively.

From the VMI-model calculations Eq. (2.5), the same basic pattern of the four bands is obtained (Fig. 2) as compared with the experimentally known data for ^{162}Hf. It was found that the agreement between the predicted and experimental energy levels for the S.b is very good. The levels ($12 \leq I \leq 26$) are fitted with the parameters (E_o = 1.768 MeV, A = 0.00843) and their values of (Eo = 2.806 MeV, A = 0.00695) were fitted into the states of spin 28^+

Table (1): The parameters a,b,c of the cubic polynomial Eq. (2.8) for ^{162}Hf (in KeV).

Band	I	Parameter		
		a	b	c
g.s	$\leq 10^+$	96.7	24.5	-0.79
S.b	$12 \rightarrow 40^+$	246.2	- 0.318	0.0775
(-,0)	$4^- \rightarrow 24^-$	536.5	-36.6	1.17
(-,1)	$5^- \rightarrow 21^-$	428.8	-25.1	0.89

Table (2): Comparison of theoretical and experimental level energies for the various bands in ^{162}Hf.

(i) Positive Parity Bands.

I^{π}	g.s. band			S. band		
	x Exp. (Mev)	Cubic poly.	VMI-model	x Exp. (MeV)	Cubic poly.	VMI-model
0^+	0	0				
2	0.285	0.285				
4	0.730	0.729				
6	1.293	1.294				2.375
8	1.940	1.941				2.695
10	2.635	2.634				
12	3.386		3.539	3.185	3.043	3.083
14	3.997		4.012	3.567	3.598	3.538
16	4.555		4.555	4.067	4.176	4.061
18	5.168		5.168	4.652	4.781	4.651
20	5.806		5.851	5.310	5.418	5.309
22			6.604	6.035	6.089	6.034
24			7.427	6.828	6.798	6.826
26				7.689	7.650	7.686
28				8.483	8.347	8.450
30				9.279	9.194	9.270
32				10.143	10.094	10.143
34				11.074	11.051	11.077
36				12.058	12.069	12.063
38				13.101	13.151	13.106
40^+				14.178	14.302	14.204

x ref. [35].

up to a 40^+. A good agreement is observed for (-,0) band levels except 2.118 MeV, 6^- and 2.439 MeV, 8^-, see (Fig.1) (E_o = 1.442 MeV, A = 0.01018): The good agreement is shown in (Fig. 2) for the (-,1) band states of spin 5^- up to 21^- with the parameters (E_o =1.348 MeV, A = 0.0103) and states of spin 23^- up to 29^- with (E_o = 2.844 MeV, A = 0.0073). The results are listed in table (2).

C- Transition Energies

To further test the E_I-I relationship, the expression (2.9) $E_I - E_{I-2} = E_I = A + BI + CI^2$ is used. If the C term is negligible, one should obtain a linear plot of E = E vs I. The data points of the g. band lie on a smooth convex curve (Fig.3) indicating that the C term is not nigligible here.For the S-band, the C term is not required (table 1). The resulting transition energies for the various bands in ^{162}Hf are shown in (Fig. 3) with the predicted ones (Cubic Polynomial and VMI-model).A pronounced anomaly is observed for the yrast sequence (12^+, 14^+,) and (12^+), (14^+), then a smooth increase of E with spin up to I = 26^+, and from 32^+ to 38^+. The calculations predict second backbending at spin 28^+. The two negative parity bands exhibit an anomaly of the lower spin parts level spacings, while the other energy spacings show a nearly monotonic increase with spin up to 20^-, (-,0) band and 21^-, (-,1) band.

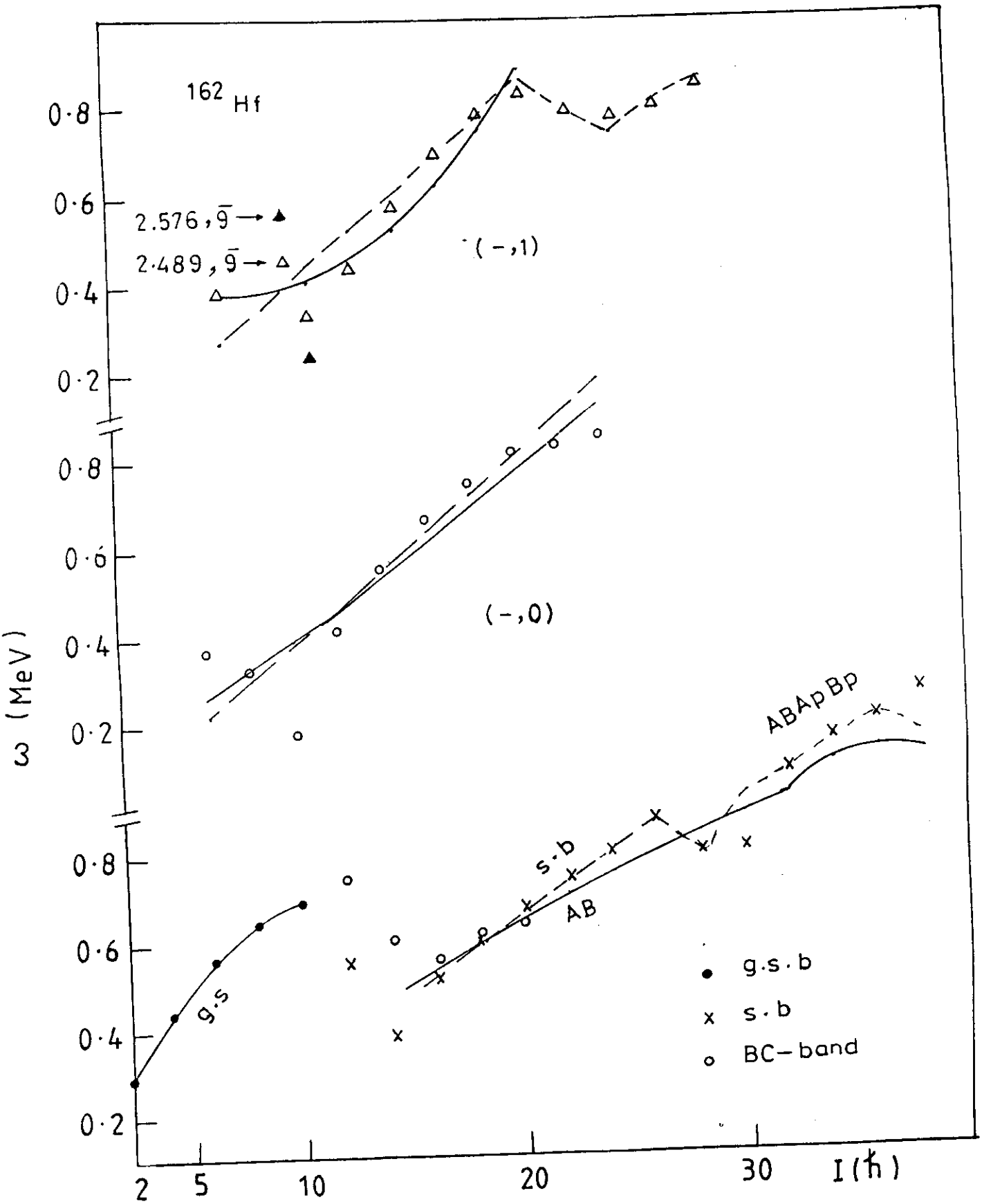

Fig. 3: Plots of cascade γ-ray energies of the observed bands in ^{162}Hf. The spin values corres pond to the upper level. The dashed lines represent the results of the model calculations.

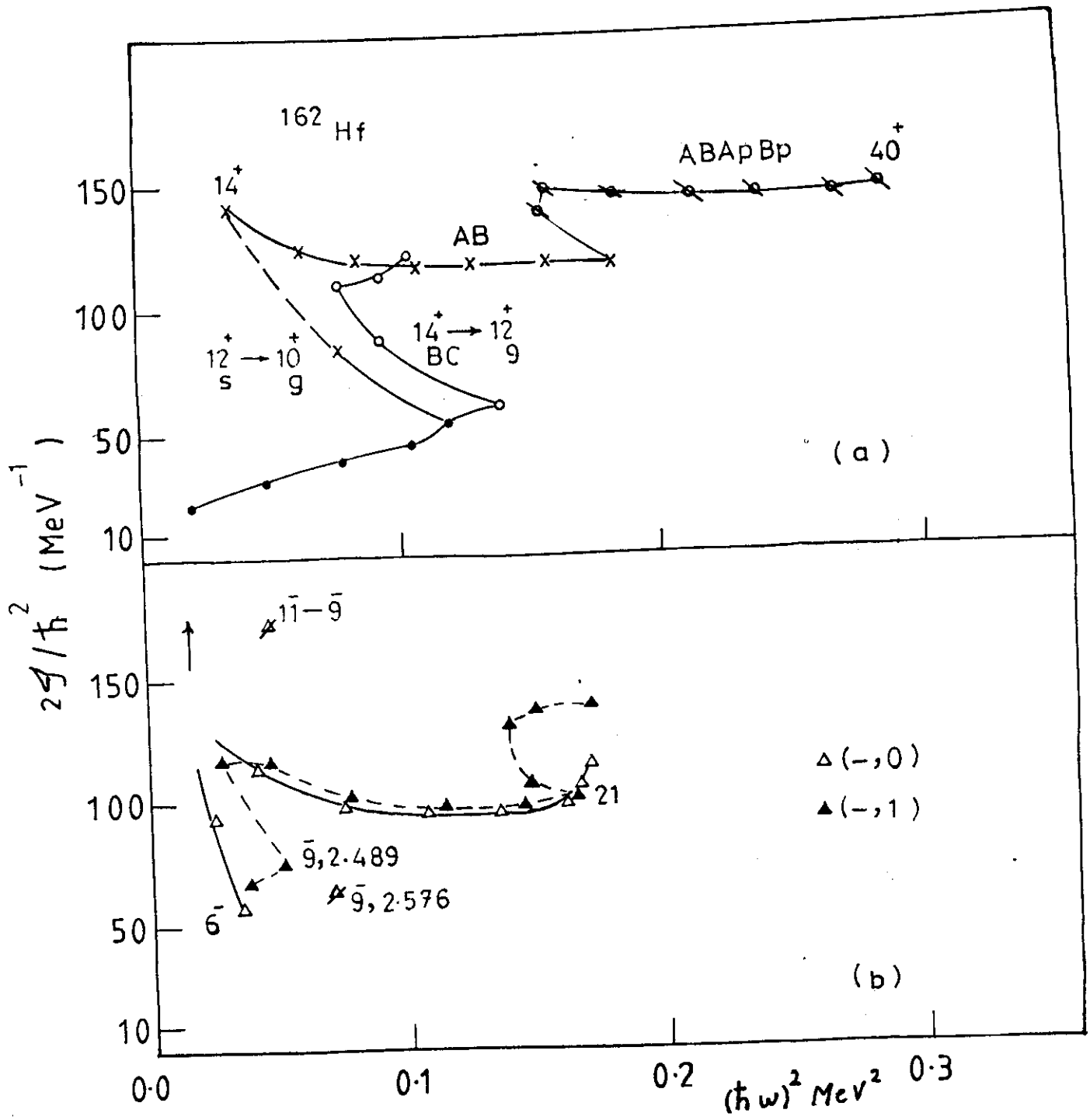

Fig. 4: Plots of moment of inertia versus the square of the ratational frequency for the various bands in ^{162}Hf.

D- Moments of Inertia

It is interesting to compare the various bands in terms of the moment of inertia vs. the square-of the rotational frequency plot. For the g.s band and S. band which crosses it, as shown in (Fig. 4), the points 12^+ and 14^+ deviate from the smooth extrapolation of the lower points of the g.s band. This effect is the first backbending due the band crossing between g.s.b and the superband. The same behavior is appeared at the points 28^+ and 30^+ which is the second backbending, which provide evidence of a second even-spin-even parity band lying above the yrast band. The other even-spin even parity-BC-band is shown in (Fig. 4-a). The moment of inertia displayed is showing another band crossing with the g.s. band.

Of particular interest is the behavior of the moment of inertia plots for the (-,0) and (-,1) bands shown in (Fig. 4-b). The transitions of the odd-and even-sequences cascades ($12^- \leq I \leq 20^-$ and $13^- \leq I \leq 21^-$) respectively, fall on a relatively smooth curves. The even spin 6^-, 8^-, 10^-, members and the odd spin 7^-,9^-,11^- members show considerable deviation from the smooth curves. The observed perturbations could be explained by the mixing of the lower portion of the (-,0) band to the lower levels of the (-,1) band. Another mixing of the level 2.623 MeV, 10^- with the level 2.635 MeV, 10^+g could explain the drastic change at point 10^-. The behavior of the higher members of the (-,1)

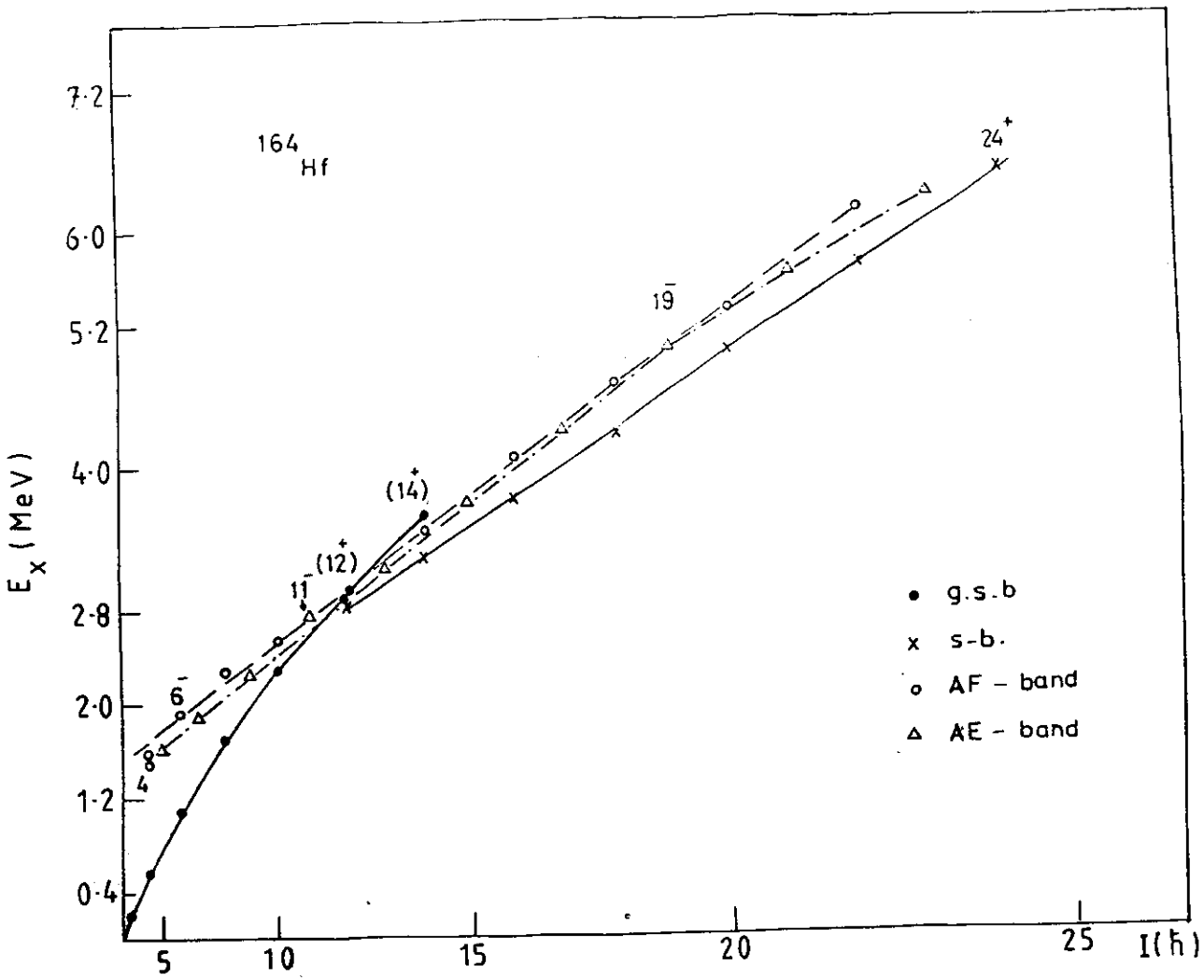

Fig. 5: Various Bands of ^{164} Hf Plotted as E_x Versus I (I+1)

band $23^-, 25^-, 27^-$ and 29^- can be explained by another crossing with the high moment of inertia yrast band.

II.3- Observed Bands in ^{164}Hf :

A- The Energy Spectrum

High spin states of ^{164}Hf have been populated in the reactions $^{148,150}Sm$ ($^{20,22}Ne$, xn) $^{163-165}Hf$ with $^{20,22}Ne$ beams of 106-117 MeV [33], and ^{120}Sn (^{48}Ti, 4n) ^{164}Hf with ^{48}Ti beam of 225 MeV [36]. Plots of the various bands in E_x versus I (I + 1) space are shown in (Fig. 5).

A.1- Positive Parily Levels :

The positive parity yrast sequence in ^{164}Hf has been observed up to 8.433 MeV, 28^+ [36] and extended up to 11.162 MeV, (34^+) [33]. The placements of the highest three levels of 9.323, 10.179 and 11.162 MeV with assignments (30^+), (32^+) and (34^+) into the level scheme remain uncertain [33]. Two levels of 2.995 MeV, (12^+) and 3.619 MeV, (14^+) were interpreted as a continuation of the ground band beyond the crossing with the S. band [33].Some of differences appeared in the structure of the negative parity bands. Most of these differences will taken into account in this analysis.

A.2- Negative Parity Levels :

The begining of the (-,0) band is 1.5203 MeV, 4^- [36] or 1.614 MeV, $(4^-,5^-)$ as in [33]. The level of the same energy 1.521 MeV is assigned 5^-, and considered as the begining of the (-,1) band [33]. From the I(I+1) plot, (Fig. 5), it has included the 1.614 MeV, 5^- (not observed in [36]) in the (-,1) band. The agreement between the two previous works is completely for the remaining states of the (-,1) band. The (-,0) band extended up to 9.215 MeV, (30^-) [33] or 10.187 MeV, (32^-) [36].

B- The Predicted Energy Levels

Since ^{164}Hf is a transitional nucleus with $R_{42} = 2.78$, a plot of E_x vs I may be more appropriate (Fig.6).The band grouping is clearly visible on this plot. The levels of 2.995 MeV, (12^+) and 3.619 MeV, (14^+) are on the smooth curve through the levels of the g.s. band. The level of 1.614 MeV, 5^- is appeared as expected, as the begining of the (-,1) band. Table (3) lists the values of the parameters a,b,c (Eq. 2.8). The results of the VMI-model calculations are listed in table 4. The energy levels reproduced very well except the three highest ones. The results are shown in (Fig. 5) as compared with the experimental data. The parameters used are $\mathcal{J}_o$ = 19 MeV^{-1}, C = 0.00051) for g.s band and (E_o = 1.295 MeV, A = 0.00868) for S.band.

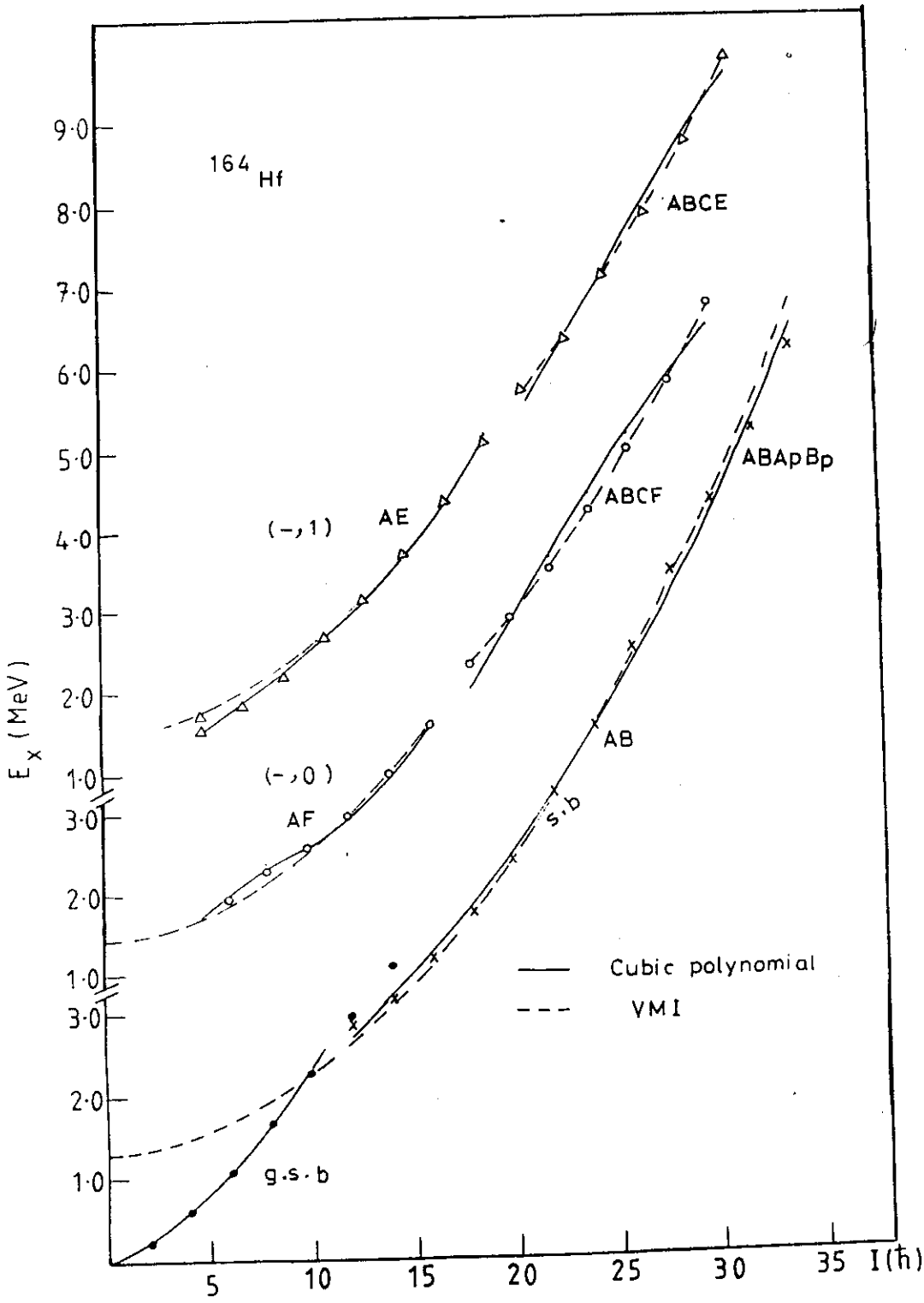

Fig. 6: Plot of the level excitation energies (E_x) as a function of spin I for various bands in ^{164}Hf connected by a theoretical curves.

Table (3): The parameters a,b,c of the cubic polynomial Eq. (2.8) for ^{164}Hf (in KeV).

Band	I	Parameter		
		a	b	c
g.s	≤ 10	58.36	25.2	-0.8
S.b	$12 \leq I \leq (34)$	225.4	- 1.45	0.138
(-,0)	$4^- \leq I \leq 16^-$	571	-51.6	2.01
	$18^- \leq I \leq (30^-)$	0.19	20	0.34
(-,1)	$5^- \leq I \leq 19^-$	385	-22	0.838
	$21^- \leq I \leq (31^-)$	0.051	17.9	-0.257

Table (4): Comparison of theoretical and experimental level energies for the various bands in ^{164}Hf.

(i) Positive Parity Bands.

I^{π}	g.s. band			S. band		
	x Exp. (Mev)	Cubic poly.	VMI-model	x Exp. (Mev)	Cubic poly.	VMI-model
0^+	0	0	0			
2	0.211	0.211	0.238			
4	0.587	0.586	0.637			
6	1.085	1.085	1.133			
8	1.669	1.671	1.704			
10	2.305	2.304	2.334			
12	2.995			2.872	2.735	2.649
14	3.619			3.211	3.251	3.117
16				3.679	3.801	3.655
18				4.263	4.393	4.263
20				4.940	5.032	4.940
22				5.700	5.726	5.687
24				6.545	6.482	6.503
26				7.459	7.305	7.388
28				8.436	8.202	8.343
(30)				9.323	9.181	9.367
(32)				10.179	10.247	10.460
$(34)^+$				11.162	11.407	11.623

x ref. [33].

(ii) Negative Parity Bands (^{164}Hf)

I^{π}	(-,0)			I^{π}	(-,1)		
	x Exp. (Mev)	C.P.E.	VMI-model		x Exp. (Mev)	C.P.E.	VMI-model
3^-	1.073						
(4)	1.614	1.589	1.629				
(5)	1.614			5^-	1.521	1.480	1.727
6	1.947	2.006	1.845	7	1.836	1.903	1.972
8	2.302	2.301	2.139	9	2.245	2.291	2.291
10	2.576	2.568	2.511	11	2.699	2.683	2.686
12	2.962	2.906	2.962	13	3.156	3.119	3.156
14	3.494	3.411	3.491	15	3.701	3.641	3.701
16	4.131	4.179	4.098	17	4.336	4.288	4.321
18	4.766	4.534	4.775	19	5.010	5.099	5.016
20	5.359	5.326	5.349	21	5.670	5.523	5.640
22	5.982	6.116	5.981	23	6.336	6.353	6.321
24	6.673	6.887	6.672	25	7.063	7.184	7.063
26	7.443	7.625	7.422	27	7.873	8.005	7.865
28	8.292	8.312	8.230	29	8.764	8.802	8.728
$(30^-$	9.215	8.931	9.097	(31^-)	9.726	9.564	9.652

x ref. [33]

C- Transition Energies

The resulting transition energies for the various bands are shown in versus I plot (Fig. 7). The yrast band exhibit an anomaly of (12-->14-->16) level spacings, then a smooth increase of E_I with spin up to $I = 28^+$, the region of the second backbending. The first one occurs around $10^+ \leq I \leq 14^+$. Anamoly is observed for the (-,0) around (8^- - 10^- - 12^-) and another one around (7^- - 9^- -11^-) for the (-,1) band. The energy spacings show a monotonic increase with spin of above spin of 12^- and 11^-, respectively, for each band. These anomalies support the idea of mixing between the various bands.

D- Moments of Inertia

Evidence for the mixing between bands which can be found in the level spacings can be explained by the more understanding way where $2\mathcal{J}/\hbar^2$ is plotted versus $(\hbar\omega)^2$. The perturbations of the levels of the three bands, as well as those of the g.s. band in the region between 6 and 16 $\hbar$ can be seen clearly in (Fig. 8). The major perturbations around (8-10-12) may be explained as crossing of the (-,0) band and mixing with both the (-,1) and g.s.bands in ^{164}Hf From the level separations the upper limit on the interaction strength between (AF-g.s.b, I=12) $\leq$17 KeV. The mixing appeared from states of 2.302 MeV, 8^-, 2.245 MeV, 9^- and 2.305 MeV, 10^+. The second crossing through the yrast band is observed around [$(\hbar\omega)^2 \simeq 0.28$ MeV^2, $\hbar\omega \simeq 0.46$ MeV, $I \simeq 28^+$].

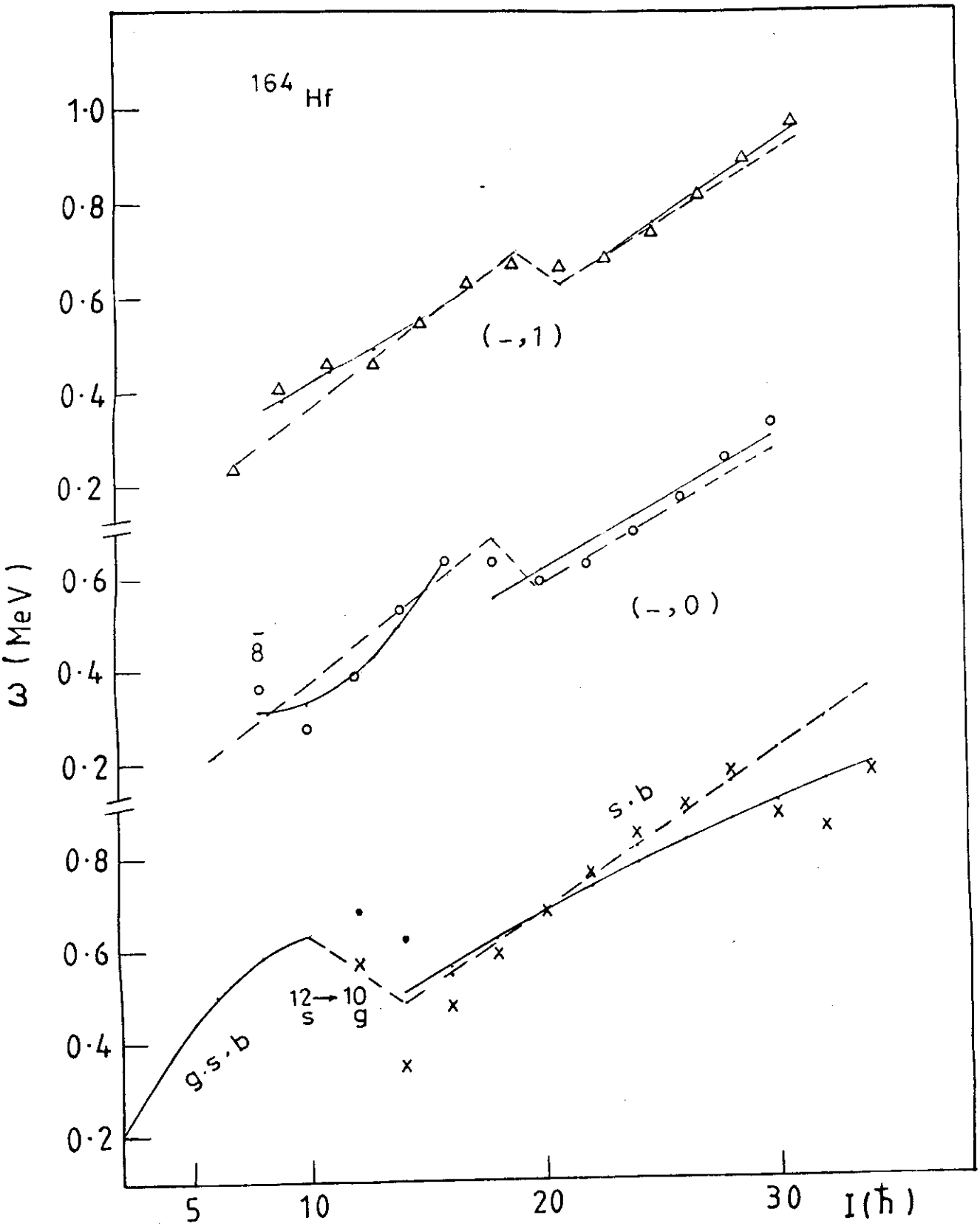

Fig. 7: Plots of cascade γ-ray energies of the observed bands in ^{164}Hf. The spin values correspond to the upper level. The dashed lines represent the results of the model calculations.

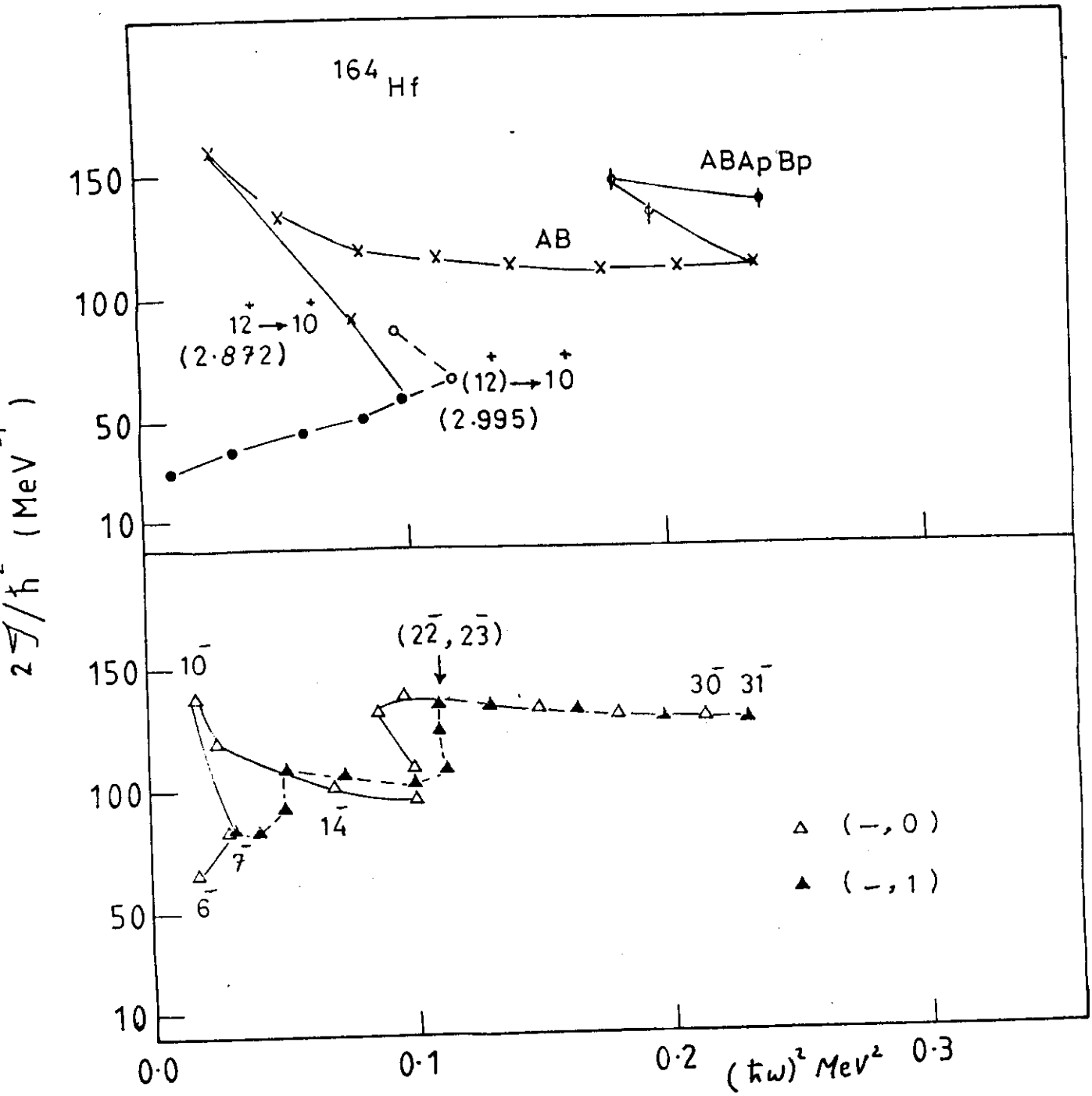

Fig. 8: Plots of moment of inertia versus the square of the ratational frequency for the various bands in ^{164}Hf.

The crossings for the negative parity bands are observed around [$(\hbar\omega)^2 \simeq 0.1$ (MeV)^2, $\hbar\omega \simeq 0.31$ MeV, $16^- \leq I \leq 18^-$ and $(\hbar\omega)^2 \simeq 0.11$ (MeV)^2, $\hbar\omega \simeq 0.33$ MeV, $19^- \leq I \leq 21^-$].

II.4- Observed Bands in ^{166}Hf :

A- The Energy Spectrum

In ^{166}Hf the yrast band (+,0) and one side band (-,1) were known [32] up to the 22^+ and 21^- states. Both these sequences are extended to appreciably higher spins (34^+) and (33^-) respectively [33]. In adition a second negative parity side band is identified up to 9.991 MeV, (32^-). An extention of the ground band is founded beyond the first band crossing up to spin 22^+. The assignments for the lower levels 1.466 MeV, (5^-), 1.552 MeV, (5^-) and 1.841 MeV, (6^-,7^-) are not accurate [33]. These bands are plotted in E_x versus I (I +1) space as shown in (Fig. 9). From the plot, the level 1.552 MeV may included as a member of (-,0) band with 4^-, and the 1.466 MeV 5^- level on the smooth line through the (-,1) members.

B- The Predicted Energy Levels

It should be interesting to apply the cubic polynomial Eq. (2-8) and VMI-model along the states of the various bands in ^{166}Hf, the transitional nucleus with $R_{42} = 2.975$. Fig. (10) shows the calculated and observed states.One can

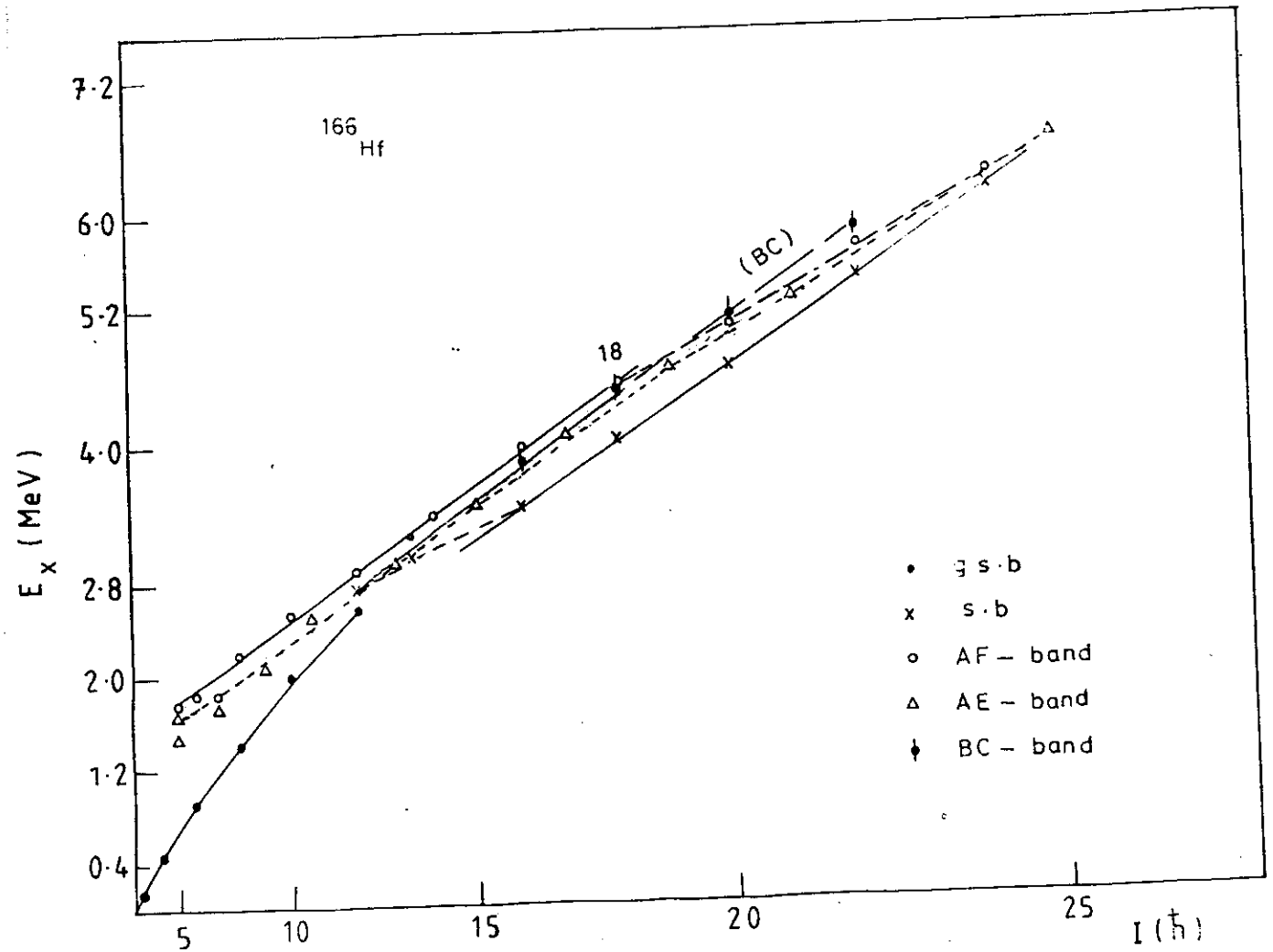

Fig. 9: Various Bands of ^{166}Hf plotted as E_x Versus I (I+1)

Table (5): The parameters a,b,c of the cubic polynomial Eq. (2-8) for ^{166}Hf (in KeV).

Band	I	Parameter		
		a	b	c
g.s	≤ 12	43.3	19.5	0.36
S.b	$14^- \leq I \leq 34^-$	168	1.97	0.072
(-,0)	$6^- \leq I \leq 18^-$	437.6	-28	0.99
	$20^- \leq I \leq 32^-$	0.134	16.5	-0.218
(-,1)	$5^- \leq I \leq 19^-$	376	-23.1	0.86
	$21^- \leq I \leq 33^-$	0.0725	15.4	-0.185

Table (6): Comparison of theoretical and experimental level energies for the various bands in ^{166}Hf.

(i) Positive Parity Bands.

I^{π}	g.s. band			S. band		
	$x_{Exp.}$ (Mev)	Cubic poly.	VMI-model	$x_{Exp.}$ (Mev)	Cubic poly.	VMI-model
0^+	0	0	0			
2	0.158	0.162	0.145			
4	0.470	0.462	0.451			
6	0.897	0.883	0.876			
8	1.406	1.409	1.394			
10	1.972	2.021	1.990			
12	2.735	2.701	2.650	2.566**		
14	3.211		3.282	3.009	2.937	2.953
16	3.835		3.835	3.449	3.488	3.449
18	4.459		4.458	4.009	4.084	4.009
20	5.122		5.150	4.671	4.726	4.633
22	5.852		5.920	5.410	5.419	5.321
24				6.201	6.165	6.073
26				7.030	6.969	6.888
28				7.895	7.834	7.769
30				8.801	8.763	8.713
32				9.753	9.759	9.721
$(34)^+$				10.747	10.827	10.793

x ref. [33].
** from the present analysis

(ii) Negative Parity Bands (^{166}Hf)

I^π	(-,0)			I^π	(-,1)		
	$x_{Exp.}$ (Mev)	C.P.E.	VMI-model		$x_{Exp.}$ (Mev)	C.P.E.	VMI-model
4^-	1.552**		1.743				
(6)	1.841	1.829	1.932	5^-	1.466**	1.413	1.548
(7)	1.841			7	1.726	1.802	1.790
8	2.197	2.211	2.189	9	2.079	2.150	2.106
10	2.540	2.560	2.516	11	2.497	2.501	2.497
12	2.911	2.921	2.911	13	2.962	2.895	2.962
14	3.375	3.344	3.375	15	3.473	3.373	3.501
16	3.921	3.875	3.907	17	4.030	3.977	4.115
18	4.516	4.561	4.508	19	4.625	4.748	4.803
20	5.090	4.861	4.978	21	5.253	5.096	5.221
22	5.679	5.671	5.637	23	5.927	5.918	5.913
24	6.357	6.497	6.357	25	6.665	6.761	6.666
26	7.138	7.330	7.138	27	7.481	7.616	7.482
28	8.018	8.159	7.980	29	8.375	8.476	8.358
(30)	8.980	8.973	8.880	(31)	9.338	9.330	9.296
$(3\bar{2})$	9.991	9.762	8.848	(33)	10.330	10.171	10.296

x ref. [33]
** from the present analysis

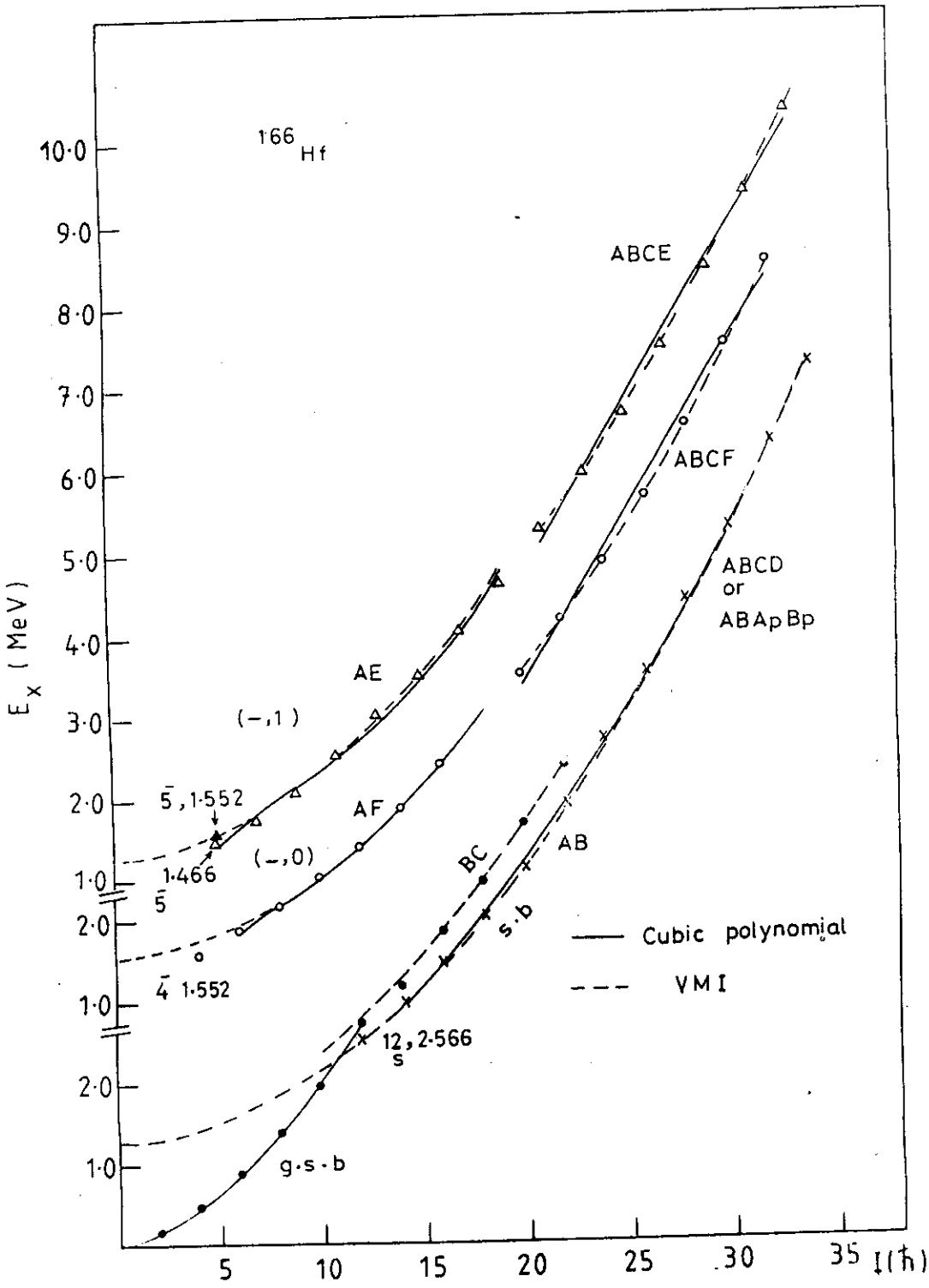

Fig.10: Plot of the level excitation energies (E_x) as a function of spin I for various bands in ^{166}Hf connected by a theoretical curves.

note that the agreements between the calculated (C.P.E. and VMI) and the observed energy levels are, in general, quite good. The low spin states can be well reproduced. The begining of S.b. is appeared to be the 2.566 MeV, 12^+ level. The high-spin states nicely described by the VMI-model calculations. Table (5) lists the values of the parameters a,b,c.The vibrational and rotational structures are clearly shown where $a \neq b$. The comparison of values of the term "a", 43.3 for ^{166}Hf, 58.36 for ^{164}Hf and 96.7 for ^{162}Hf is consistent with the increased $R_{42} = E_4/E_2$ ratios of 2.56, 2.78 and 2.975 in the g.s. bands. The results obtained are given in table (6).The parameters used are $\frac{\hbar^2}{2J_o} = 39.6$ Mev^{-1}, C=0.00075 (g.s), E_o = 1.273 MeV, A=0.0080 (S.b), E_o = 1.571 MeV, A=0.00859 (AE), E_o= 1.763 MeV, A = 0.00766 (ABCE), E_o = 1.278 MeV, A = 0.0093 (AF) and E_o = 1.676 MeV, A = 0.00769 (ABCF).

C- Transition Energies

Transition energies for various bands are displayed in (Fig. 11). The difference between the experimentally known transion energies and the fitted energies cannot be neglected in the region for $I_s \geq 12^+$, above the first band crossing. For $I_s \geq 12^+$, the experimental energies are above that with the fitted energies.The reason for these deviations is the mixing between the levels in the spin range $12^+ - 22^+$.

The resulting transition energies for the bands (-,0) and (-,1) are shown in (Fig. 11). An anomaly of 18^- to 22^- and of 19^- to 23^- level spacings support the idea of band crossing and mixing [(AF --> ABCF) and (AE --> ABCE)] respectively.

D- Moments of Inertia

A pronounced anomaly is observed for the even spin even parity bands in ^{166}Hf around spin region (12^+, 14^+, 16^+). It is clear from (Fig. 12), that band crossings occurred in this region. The second crossing (upbending) occurred around spin of 26^+.

The negative parity bands are both plotted in (Fig.11). Although the two bands level off at a moment of inertia near that of the even spin positive parity yrast band, the moment of inertia of the (-,1)band is apparently considerably lower for $I \leq 21^-$.The value of $2\mathcal{J}/\hbar^2$ increases gradually with $(\hbar\omega)^2$ for $9^- \leq I \leq 21^-$. The lower part for the (-,0) band members, ($I \leq 22^-$), show considerable deviation from a smooth curve. The observed perturbations could be explained by interactions between the lower members of the two negative bands. The observed levels 12^-,2.911 MeV and 10^-,2.540 MeV with 371.3 KeV interband transition may be interpreted as band crossing with the two levels 13^-,2.962 MeV and 11^-, 2.497 MeV with interband transition of 465.4 KeV. Other causes will be discussed latter on the next chapter.

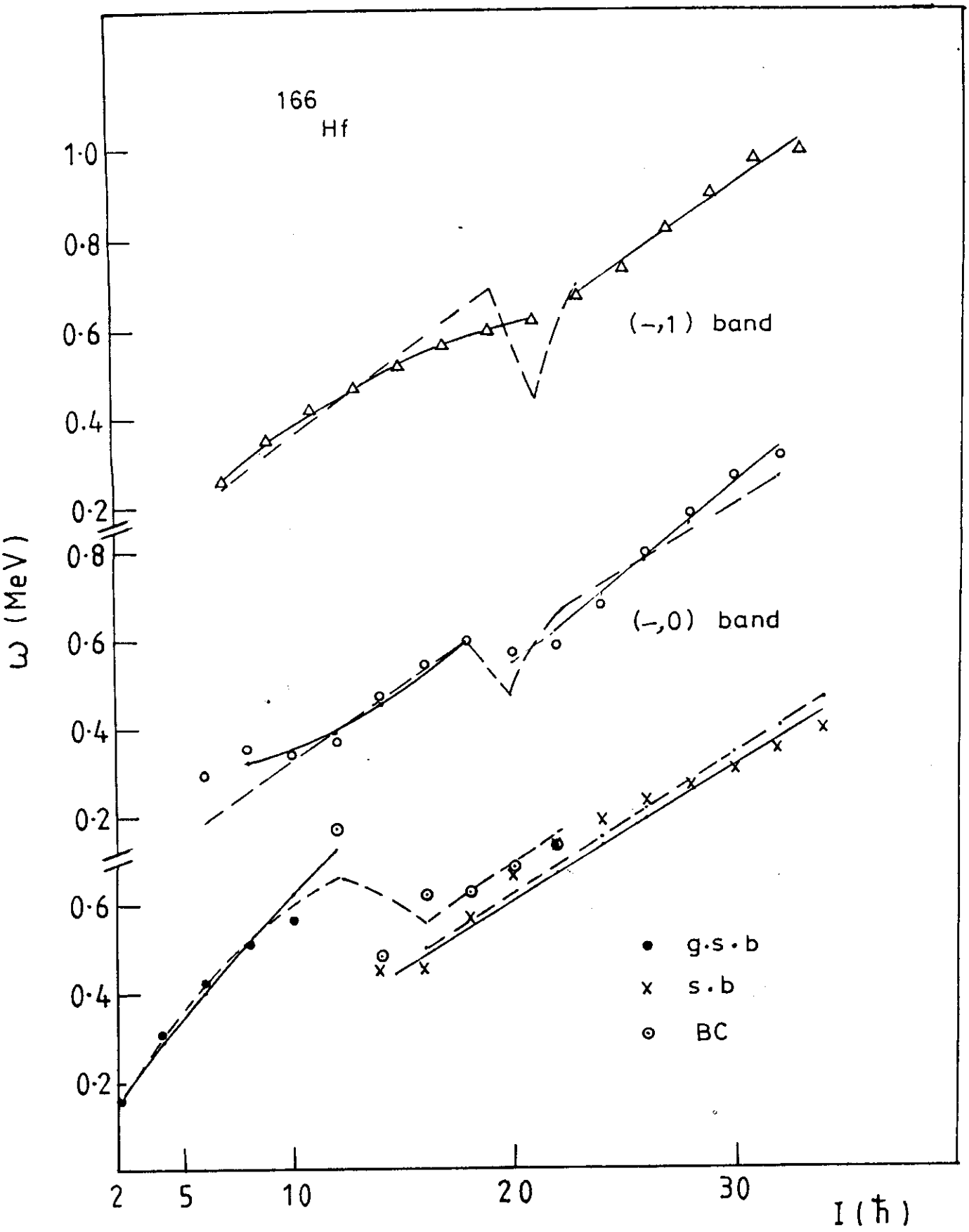

Fig.11: Plots of cascade γ-ray energies of the observed bands in ^{166}Hf. The spin values corres pond to the upper level. The dashed lines represent the results of the model calculations.

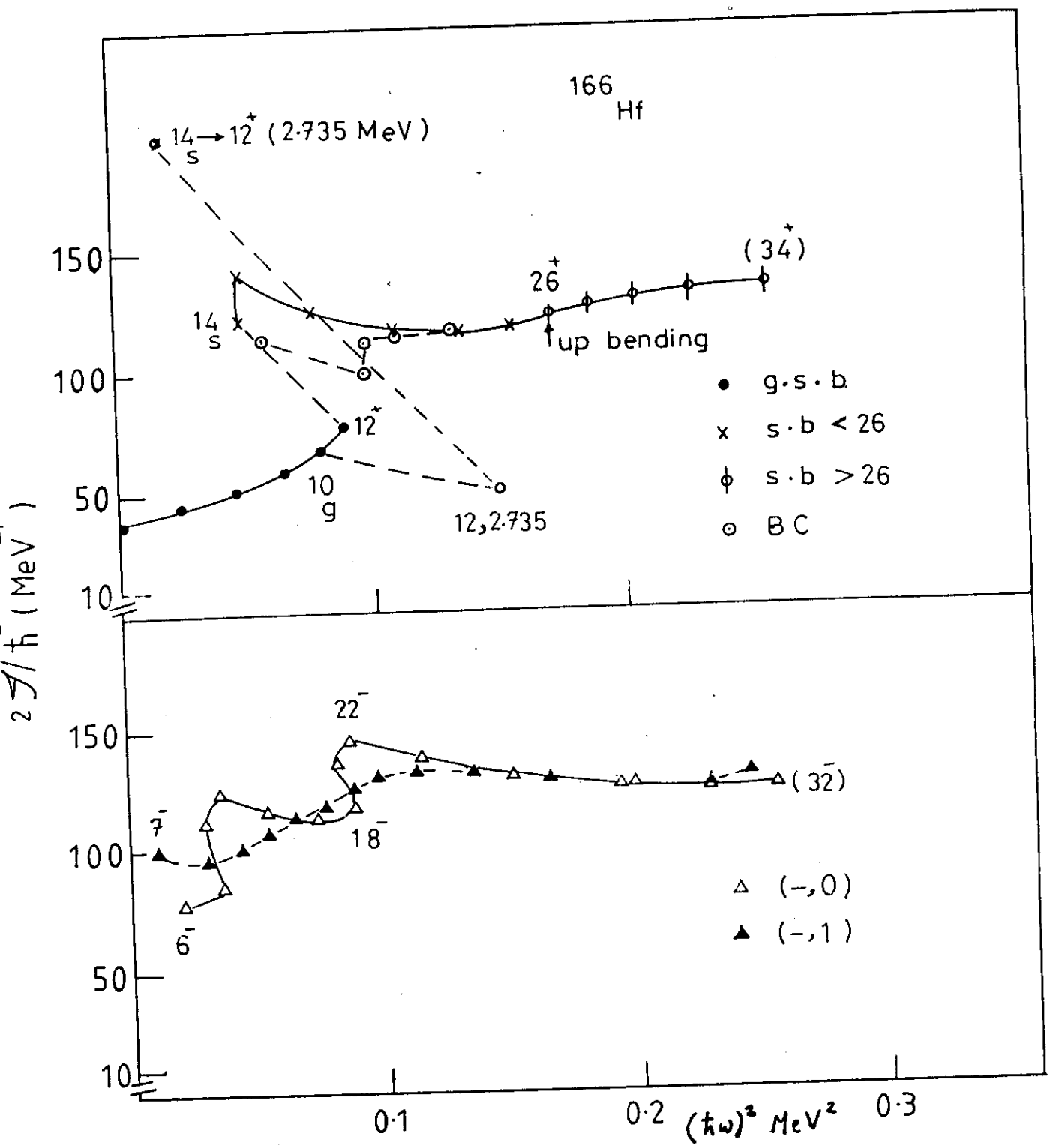

Fig.12: Plots of moment of inertia versus the square of the ratational frequency for the various bands in ^{166}Hf.

II.5- Observed Bands in ^{168}Hf :

^{168}Hf with Z=72 and N=96 is a typical mid-shell nucleus with stable quadrupole deformation. It is almost rotational with R_{42} =3.11 and behaves like a perfect rotor above spin 20 [40]. The nucleus ^{168}Hf was studied up to spin 38^+ in the yrast band and to spin 41^- and 38^- in the lowest two negative parity bands [40,41]. A new band with even spins and negative parity was found [41].

A- The Energy Spectrum

The I(I+1) dependence is characteristic for the rotation of a rigid body or the average yrast line of a Fermi gas [2].The construction of the yrast level involves a number of quasiparticles that increases linearly with I and,since the average energy of the quasiparticles is proportional to their number, the resulting total excitation energy is proportional to I^2. An analysis using the simple I(I+1) relationship for the energies of members of the bands is given in (Fig. 13). The placement of the levels as indicated in (Fig. 13), is based initially on the connecting inband transitions.

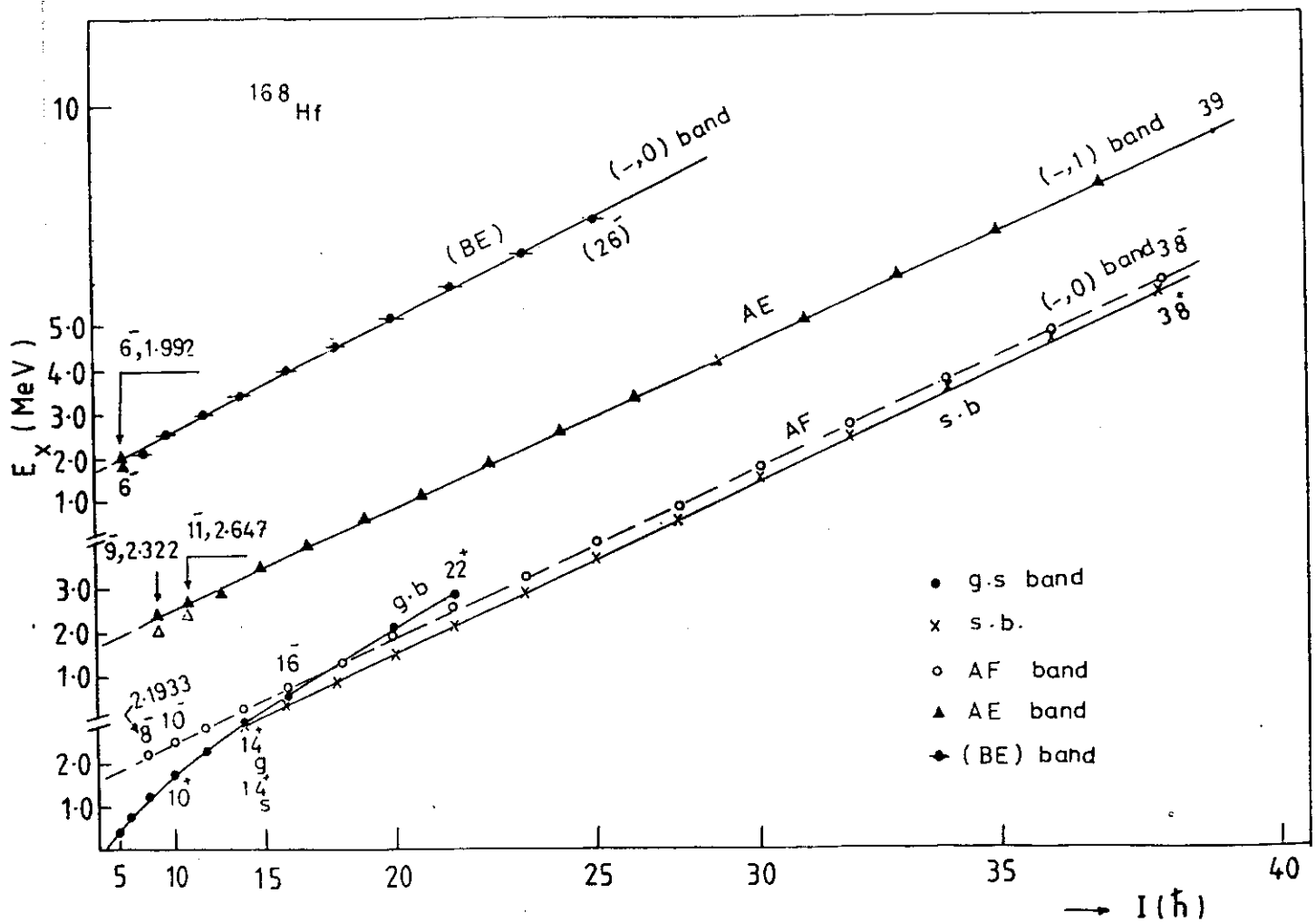

Fig.13: Various Bands of ^{168} Hf plotted as E_x Versus I (I+1)

A.1- Positive Parity Levels :

The nucleus ^{168}Hf was known up to spin 22^+ in the ground-state band and (34^+) in the yrast band [40]. The yrast band is extended (tentatively) to spin 38[41]. The levels display a consistent decay pattern, and lie on the line in E_x versus I(I+1).

A.2- Negative Parity Levels :

The even spin levels, AF band, based on 2.193 MeV, 8^-[41] form a sequence with smooth behavior in E_x versus I(I+1) space. The 2.1548 MeV, 8^- level [40] lies down the line, (Fig. 13). The odd-spin members decay only to the ground state band, they are easily placed in E_x versus I(I+1) space, above spin 13^-, 2.938 MeV. The 2.322 and 2.647 MeV were both tentatively assigned (9^-) and (11^-) respectively [41]. These two levels are proposed in the present work as members of the (-,0) band by virtue of their positions in E_x versus I(I+1) space. They are replaced the two levels 2.066 MeV, 9^- and 2.474 MeV, 11^- [40]. The third negative parity band (BE) [41] form a sequence with smooth behavior in E_x versus I(I+1) space except its begining the 1.813 MeV 6^- which lies below the straight line (Fig. 13).

Table (7): Comparison of theoretical and experimental level energies for the various bands in ^{168}Hf.

(i) Positive Parity Bands

I^{π}	g.s. band		S. band	
	$x_{Exp.}$ (Mev)	VMI-model	$x_{Exp.}$ (Mev)	VMI-model
0^+	0	0		
2	0.1239	0.126		
4	0.3854	0.388		
6	0.7566	0.750		
8	1.213	1.189		
10	1.735	1.692		
12	2.305	2.298		
14	2.938	2.852	2.857	
16	3.623	3.499	3.309	
18	4.322	4.183	3.832	
20	5.049	4.903	4.439	
22	5.814	5.655	5.124	
24			5.875	
26			6.687	
28			7.562	
30			8.500	
32			9.499	
34			10.549	
36			11.637	
38^+			12.742	

x refs. [40,41]

(ii) Negative Parity Bands in ^{168}Hf

I^π	(-,0)		I^π	(-,1)		I^π	(-,0) **	
	$x_{Exp.}$ (Mev)	VMI-model		$x_{Exp.}$ (Mev)	VMI-model		Exp (Mev)	VMI-model
						6^-	1.813	1.998
8	2.155, 2.193 [1)]	2.267				8	2.155	2.258
10	2.466	2.554	9^-	2.0663, 2.322 [2)]	2.441	10	2.553	2.587
12	2.827	2.902	11	2.474, 2.647 [2)]	2.750	12	2.977	2.985
14	3.268	3.309	13	2.938	3.119	14	3.453	3.453
16	3.777	3.778	15	3.442	3.546	16	3.990	3.990
18	4.335	4.307	17	3.990	4.033	18	4.580	4.596
20	4.933	4.896	19	4.578	4.577	20	5.215	5.272
22	5.574	5.547	21	5.198	5.182	22	5.896	6.016
24	6.268	6.257	23	5.854	5.845	24	6.630	6.830
26	7.029	7.028	25	6.567	6.566	26^-	7.425	7.713
28	7.860	7.859	27	7.348	7.348			
30	8.763	8.751	29	8.199	8.188			
32	9.731	9.703	31	9.115	9.086			
34	10.756	10.715	33	10.092	10.044			
36	11.829	11.788	35	11.119	11.061			
38^-	12.933	12.922	37	12.181	12.136			
			39	13.257	13.270			
			41^-	14.345	14.464			

** ref [41]

x refs [40,41]
1) ref [40]

x refs. [40,41]
2) present analysis

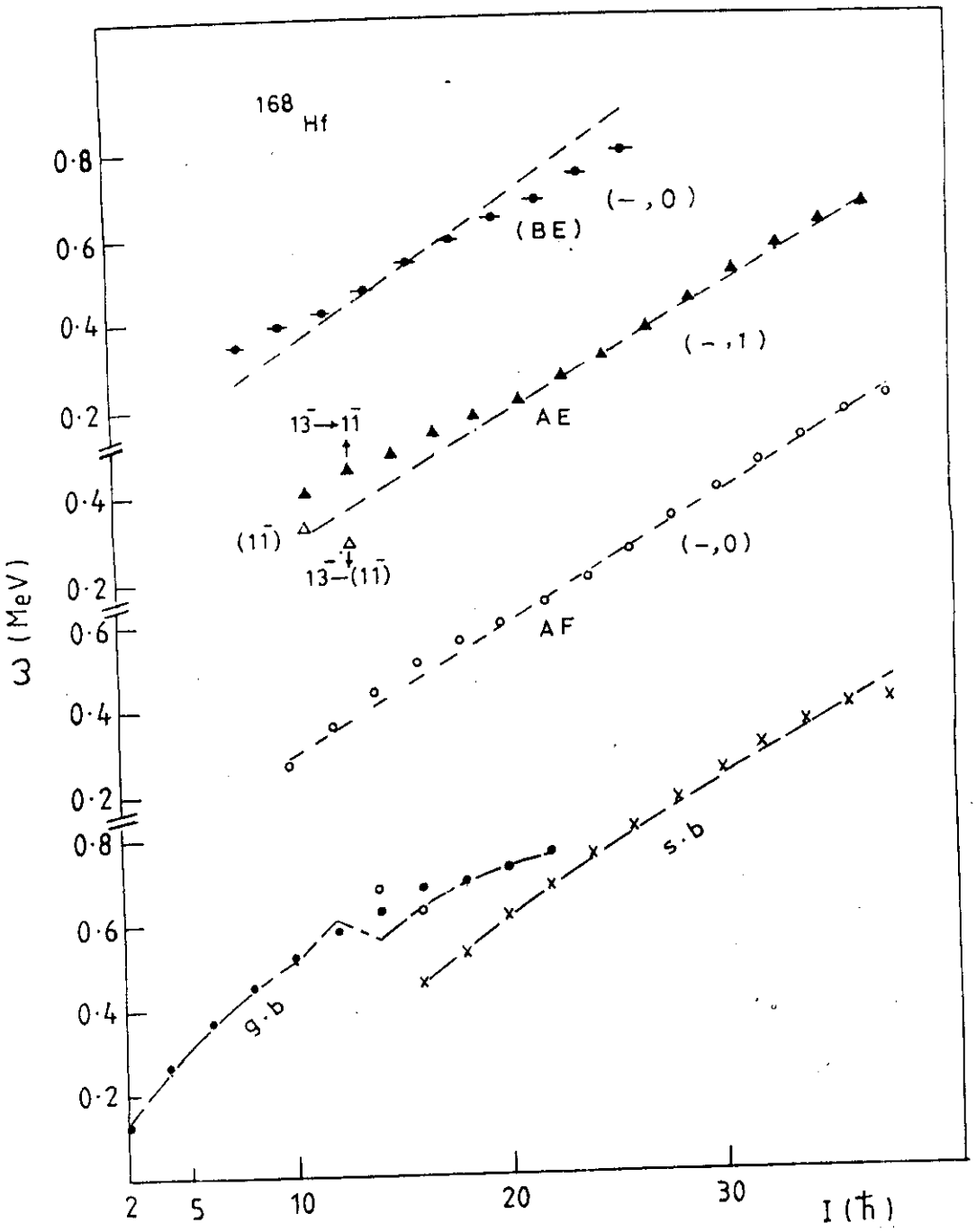

Fig.15: Plots of cascade γ-ray energies of the observed bands in ^{168}Hf. The spin values corres pond to the upper level. The dashed lines represent the results of the model calculations.

above the predicted line. The deviation appears partially through the energy spacings of the(-,1) band for $11^- \leq I \leq 17^-$ and disappeared completely for $19^- \leq I \leq 37^-$.

The considerable discrepancy as it is shown in (Fig. 15), for the new band [41] may be due to the perturbation of closely spaced levels having the same spin ((BE) and AF-band) which interact.

D- Moments of Intertia

It is interesting to compare the various bands in terms of the moment of inertia vs the square of the rotational frequency plot. The whole picture is shown in (Fig. 16). For the g.s band and the S-band which crosses it, as shown in (Fig. 16-a), the points 14 and 16 deviate from the smooth extrapolation of the lower points of the g.s. band. This effect can be explained in terms of mixing with the levels of the same spin belonging to the S-band in particular, the 14_s and 16_s. A corresponding extrapolation to higher spin reveals a similar phenomenon involving the 14_s and 16_s points. This can be taken as further evidence that the interacting levels belonging to these two bands are correctly identified.

Of particular interest is the behavior of the moment of inertia plots for the even and odd spin sequences of the two negative parity bands shown in (Fig. 16-b). The

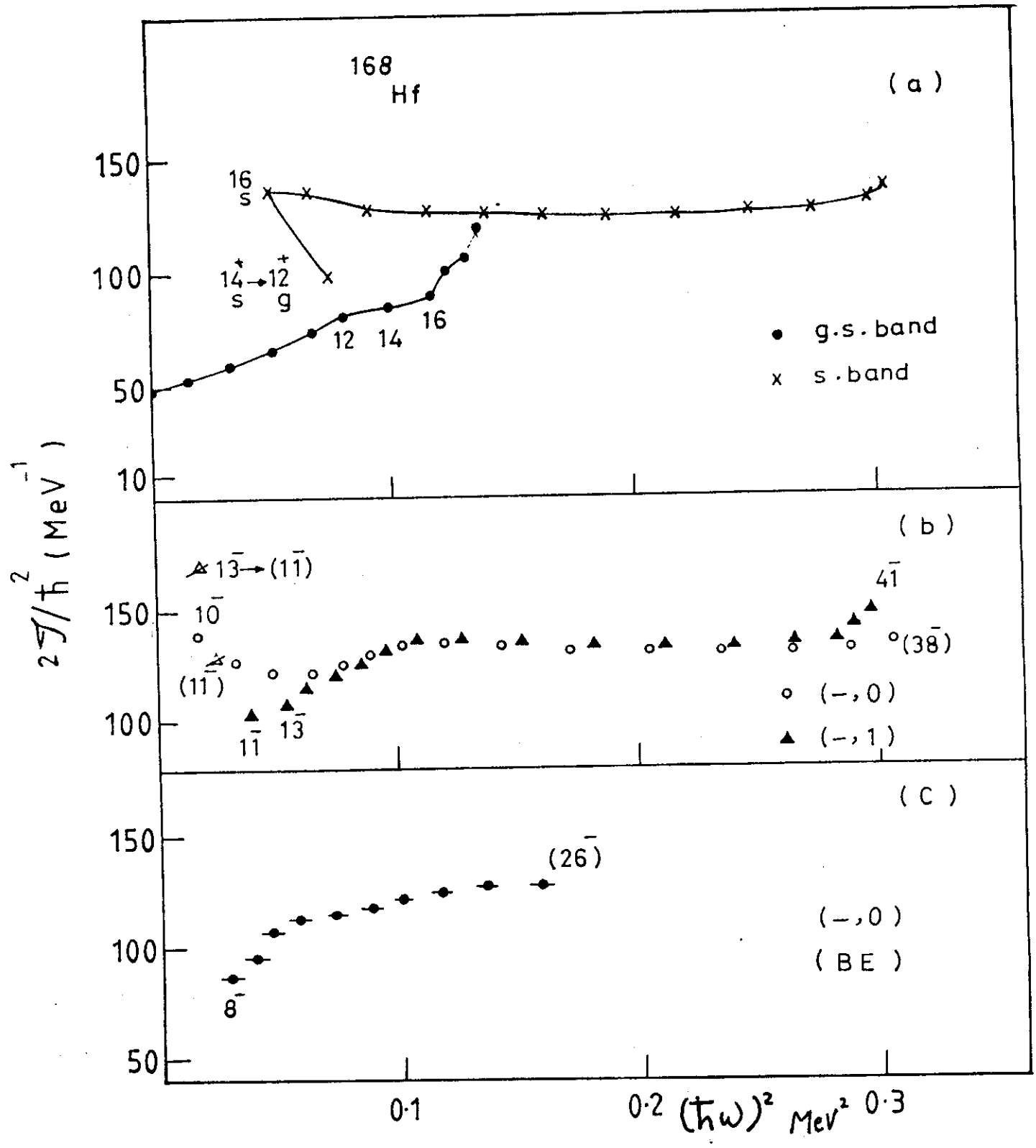

Fig.16: Plots of moment of inertia versus the square of the ratational frequency for the various bands in ^{168}Hf.

transitions of the odd-spin cascade (13^{-}-37^{-}) and even-spin cascade (14^{-}-36^{-}) fall on a relatively one smooth curve. The lower spin members show considerable deviation from the smooth curve. The observed perturbation could be explained by the mixing of the level 2.4659 MeV, 10^{-} with the level 2.4736 MeV, 11^{-}. The observed deviation for the higher spin members of the odd sequence will be explained latter on the next chapter.(CH. III) knowing that the spin assignments above 37^{-} are tentative [41].

Finally the even-spin band (the new negative band) [41] is shown in (Fig. 16-c). The moment of inertia displayed is close to that of the other negative bands.